

1995

Development of an electroplating bath for fabrication of CoNiFe thin films

Siamak Sarhadi
San Jose State University

Follow this and additional works at: https://scholarworks.sjsu.edu/etd_theses

Recommended Citation

Sarhadi, Siamak, "Development of an electroplating bath for fabrication of CoNiFe thin films" (1995). *Master's Theses*. 1030.
DOI: <https://doi.org/10.31979/etd.mpbn-4h2e>
https://scholarworks.sjsu.edu/etd_theses/1030

This Thesis is brought to you for free and open access by the Master's Theses and Graduate Research at SJSU ScholarWorks. It has been accepted for inclusion in Master's Theses by an authorized administrator of SJSU ScholarWorks. For more information, please contact scholarworks@sjsu.edu.

INFORMATION TO USERS

This manuscript has been reproduced from the microfilm master. UMI films the text directly from the original or copy submitted. Thus, some thesis and dissertation copies are in typewriter face, while others may be from any type of computer printer.

The quality of this reproduction is dependent upon the quality of the copy submitted. Broken or indistinct print, colored or poor quality illustrations and photographs, print bleedthrough, substandard margins, and improper alignment can adversely affect reproduction.

In the unlikely event that the author did not send UMI a complete manuscript and there are missing pages, these will be noted. Also, if unauthorized copyright material had to be removed, a note will indicate the deletion.

Oversize materials (e.g., maps, drawings, charts) are reproduced by sectioning the original, beginning at the upper left-hand corner and continuing from left to right in equal sections with small overlaps. Each original is also photographed in one exposure and is included in reduced form at the back of the book.

Photographs included in the original manuscript have been reproduced xerographically in this copy. Higher quality 6" x 9" black and white photographic prints are available for any photographs or illustrations appearing in this copy for an additional charge. Contact UMI directly to order.

UMI

A Bell & Howell Information Company
300 North Zeeb Road, Ann Arbor, MI 48106-1346 USA
313:761-4700 800:521-0600

**Development of an Electroplating Bath
for Fabrication of CoNiFe Thin Films**

A Thesis

Presented to

The Faculty of the Department of Materials Engineering
San Jose State University

In Partial Fulfillment
of the Requirements for the Degree
Master of Science

By

Siamak Sarhadi

May, 1995

UMI Number: 1374621

**Copyright 1995 by
Sarhadi, Siamak
All rights reserved.**

**UMI Microform 1374621
Copyright 1995, by UMI Company. All rights reserved.**

**This microform edition is protected against unauthorized
copying under Title 17, United States Code.**

UMI


**300 North Zeeb Road
Ann Arbor, MI 48103**

© 1995

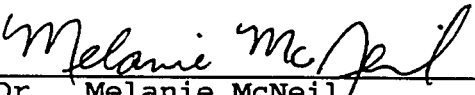
Siamak Sarhadi

ALL RIGHTS RESERVED

APPROVED FOR THE DEPARTMENT OF MATERIALS ENGINEERING


4/10/95

Dr. Emily Allen



APRIL 10, 1995

Dr. Melanie McNeil


4/10/95

Dr. Robert Rottmayer

APPROVED FOR THE UNIVERSITY



ABSTRACT

Development of an Electroplating Bath for Fabrication of CoNiFe Thin Films

By

Siamak Sarhadi

The search for high moment soft ferromagnetic material for use in thin film heads is becoming urgent as the areal density in magnetic recording approaches 1 Gbit/in². High density recording requires a high coercivity medium. In order to write on a high coercivity medium the core of the head should consist of a high moment soft ferromagnetic material. In this work a plating bath was developed for a class of ternary CoNiFe alloys which have a promise of high saturation magnetization, M_s , as well as high permeability, μ_r , low coercivity, H_c , and small magnetostriction constant, λ_s , required for a suitable core material for thin film heads. The optimum composition was found to be Co_{83.4} Ni_{5.7} Fe_{10.9}.

ACKNOWLEDGMENTS

This work has been done with the support and collaboration of Read-Rite Corporation. I would like to express my sincere appreciation to all the individuals whose help made the completion of the thesis possible.

First, I wish to express my deepest gratitude to my thesis advisor, Dr. Emily Allen, for her invaluable guidance, assistance, and providing me with the precious opportunity to engage in the research described in the thesis.

I also want to thank Dr. Melanie McNeil for serving on my reading committee and providing timely guidance in spite of her busy schedule.

My sincerest appreciation goes to Dr. Robert Rottmayer, vice president of Read-Rite Corporation, who has provided me needed advice, help and support during the course of the work. I would also like to thank many individuals in Read-Rite Corporation to whom I am deeply indebted: Vince Retort and Steven C. Rudy for their support, Satinder Singh for his invaluable assistance in preparation and processing the wafers, Inge Fernau for the chemical lab support, Michael

Murdock and Pardeep Puri for EDX analysis, Dr. Hua-ching Tong for obtaining XRD data, and Dr. Durga Ravipati for his technical support.

I also wish to express my gratitude to my parents and all my teachers in the past for their love, trust and teaching.

Finally, I thank my wife, Mahvash, for her constant love, support, encouragement and understanding my spending long hours and weekends during the course of the work.

TABLE OF CONTENTS

CHAPTER	Page
ABSTRACT	iv
ACKNOWLEDGMENTS	v
TABLE OF CONTENTS	vii
LIST OF TABLES	x
LIST OF FIGURES	xi
1. INTRODUCTION	1
1.1. Background	1
1.2. Motivation	3
1.3. Electroplating	5
1.4. Previous Work on Electrodeposition of Ternary CoNiFe Alloys	7
2. EXPERIMENTAL METHODS	16
2.1. Preparation of CoNiFe Thin Film	16
2.2. Electrodeposition of CoNiFe	16
2.3. Magnetic Characterization of Plated Thin Films	23
2.3.1. MH and BH Loops	23
2.3.2. Magnetic Units	25
2.3.3. Requirement of Thin Film Head Material	26
2.3.4. M-H Loop Tracer	26

2.4. Film Thickness, Composition, and Structural Analysis	29
2.4.1. Thickness Measurements	29
2.4.2. Energy Dispersive X-ray Microanalysis (EDX)	30
2.4.3. X-Ray Diffractometer	31
2.5. Experimental Procedure	31
2.5.1. Plating Station	31
2.5.2. Bath Makeup and Chemistry	32
2.5.3. Bath Designs	33
3. RESULTS AND DISCUSSION	37
3.1 Bath Control	37
3.1.1 Temperature	37
3.1.2 pH	38
3.1.3 Bath Chemistry	39
3.1.4 Specific Gravity	42
3.1.5 Agitation	43
3.2 Evaluation of the Plated Film	44
3.2.1 EDX Measurements of the Film Composition	45
3.2.2 MH Loop Measurements of the Plated Film	46
3.2.3 Thickness Measurements of the Plated Film	48

3.2.4 Roughness Measurements of the Plated Film	50
3.2.5 Hardness Measurements of the Plated Film	51
3.2.6 Current Density versus Composition and Magnetic Properties	54
3.2.7 XRD and Structural Evaluation	57
3.3 Modification of the Bath and Optimization of the Compositional Gradient across the Topology of Thin Film Structure	58
3.4 The Saturation Magnetostriction (λ_s) Evaluation	61
4. CONCLUSION	62
5. REFERENCES	63
6. APPENDIX: EDX data on bath modification	65

LIST OF TABLES

Table		Page
Table 1.	Basic bath composition for electrodeposition of FeCoNi	8
Table 2.	Examples of an electroplating low and high salt bath composition	14
Table 3.	Typical properties of $\text{Co}_{80}\text{Ni}_{10}\text{Fe}_{10}$ plated film	14
Table 4.	The electromotive force(emf) series	20
Table 5.	Bath makeup and chemistry	32
Table 6.	Experimental test and measurement matrix	44
Table 7.	NiFeCo NIST-standard measured on the EDX	46
Table 8.	Repeatability study of the M-H loop tracer	48
Table 9.	Hardness measurements of the plated NiFe and CoNiFe	51
Table 10.	The compositional differences for 3 and 9 mA/cm ²	59
Table 11.	EDX data and the additions of bath modification	65

LIST OF FIGURES

Figure	Page
Figure 1. Rigid disk file component	1
Figure 2. (a)the thin-film cross section, (b)planar view, (c)a double-rail film head slider, and (d)the mounted finished head to suspension and arm(HGA)	2
Figure 3. Sectional view of a thin film inductive head	6
Figure 4. Current density versus film composition	9
Figure 5. Non-magnetostrictive compositions of CoNiFe system	10
Figure 6. The B_s and H_c of CoNiFe-based thin films	11
Figure 7. The Curie temperature of CoNiFe-based thin films	12
Figure 8. Schematic diagram of plating station	23
Figure 9. Typical easy and hard direction hysteresis loops of an anisotropic film	24
Figure 10. Typical B-H loop of plated NiFe film	25
Figure 11. Schematic diagram of M-H loop tracer	27
Figure 12. Photo resist mask layout for thickness measurement	29
Figure 13. Components of a typical EDX system	30

Figure 14. Expected composition range for the plated film	34
Figure 15. Flowchart representing the methodology of the Phase II	36
Figure 16. Temperature variation of the bath for the plated test wafers	38
Figure 17. pH variation of the bath during plating some of the test wafers	39
Figure 18. Chemical analyses data	40
Figure 19. Typical MH loop traces for plated (a)NiFe and (b)CoNiFe	47
Figure 20. Measured thicknesses for the plated wafers	49
Figure 21. Cantilever deflection detection system of the AFM	50
Figure 22. Roughness analysis of NiFe	52
Figure 23. Roughness analysis of CoNiFe	53
Figure 24. The dependency of current density on the film composition	54
Figure 25. B_s of the plated film versus Electrodeposition current density	55
Figure 26. H_k of the plated film versus electrodeposition current density	55

Figure 27. Easy and hard axis coercivity versus electrodepositon current density	56
Figure 28. The XRD analysis of the CoNiFe-plated film	57
Figure 29. EDX analyses of the cross sections for 3mA/cm ² and 9mA/cm ²	59
Figure 30. Film composition versus additions during bath modifications	60

1. INTRODUCTION

1.1 Background

Data storage systems such as magnetic tape drives, magnetic hard disk drives, and magneto-optic drives are under extensive research and development because of the market demand for higher performance and larger areal density.

The key component of a hard disk drive is the head-disk assembly which typically consists of a head-slider and a spinning magnetic hard disk. The rudiments of a rotary actuator disk drive are illustrated in Figure 1.

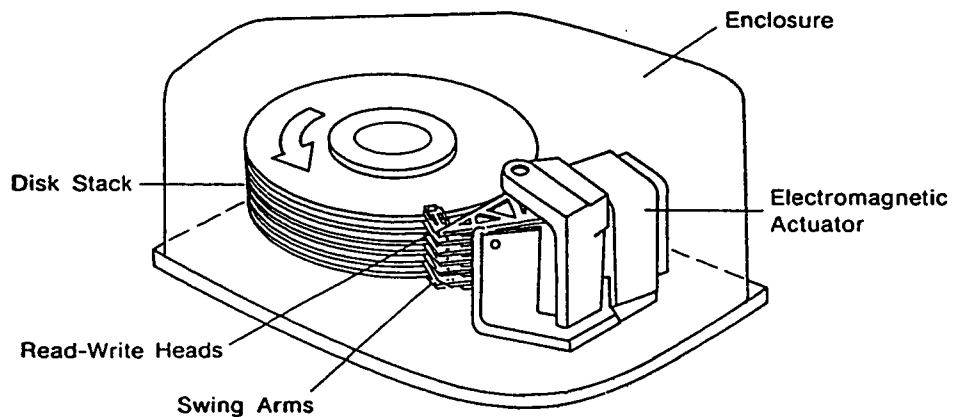


Figure 1. Rigid disk file component⁽¹⁾.

By virtue of a hydrodynamic air bearing, a constant separation called the flying height is maintained between the slider and the disk. The slider is mounted to a specially designed suspension and arm, forming the head-gimble assembly (HGA), and a magnetic recording head is located on the trailing edge of the slider. In Figure 2 a typical HGA and the representative structure of a thin film head are shown.

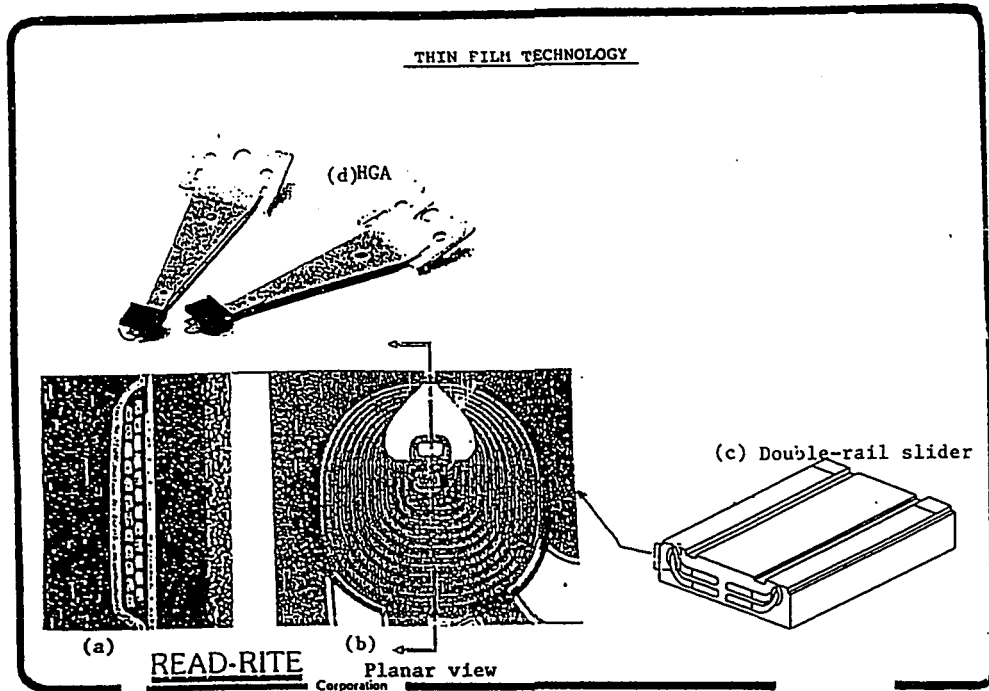


Figure 2. (a) the thin-film cross section, (b) planar view, (c) a double-rail film head slider, and (d) the mounted finished head to suspension and arm (HGA).

(courtesy of READ-RITE)

As the HGA moves along the radial direction on the disk drive the data tracks are being recorded. The multiplication of the track density by the linear data density along a track gives the areal recording density. By increasing both linear density and track density the areal recording density will increase, which will yield larger capacity, lower cost/megabyte and faster access time in disk-drives. I.B.M started using thin-film heads in disk drives in the mid-1970s, but the technology did not see significant growth until 1989 or 1990. Since then, thin-film head shipments have doubled each year. About 17 million thin-film heads were produced in 1989; about 33 million in 1990; 66 million in 1991; 117 in 1992 and about 200 million in 1993⁽²⁾.

1.2 Motivation

Several years ago, ferrite head technology supposedly reached its limits with respect to machining processes and high frequency magnetic characteristics. This started the rush toward thin film heads. Today more and more hard disk drives employ thin film recording heads which utilize polycrystalline Permalloy (approximately 81 wt.% Ni and 19 wt.% Fe, referred to as NiFe hereafter) material with a saturation magnetization (M_s) of 8×10^5 Amp/m (10,000 gauss)⁽³⁾. The high areal density in magnetic recording

requires a medium with high coercivity. On the other hand, the magnitude of coercivity, H_C , in the medium determines how densely the information can be recorded; and in order to write on a high coercivity medium the core of the head should consist of a high M_s soft ferromagnetic material. Electroplated NiFe has been the material of choice for present day thin film heads; by replacing NiFe with higher saturation magnetization material and by using high coercivity media, it will be possible to achieve both higher linear densities and higher track densities. In binary NiFe, when the Fe content is increased to achieve a greater saturation magnetization, the magnetostriction, λ_s^* , also increases. A greater λ_s is presumed to be a major contributor to read back instabilities⁽⁴⁾. Thus, a higher M_s material with a low λ_s is needed. Sputtered CoNiFe alloys (Perminvar alloy) have long been known as a soft magnetic material with high saturation magnetization exceeding twice that of Permalloy.⁽⁵⁾ However, an electroplated CoNiFe would be a convenient replacement for NiFe. Hence the motivation of this thesis is to develop a plating bath for suitable ternary CoNiFe alloy composition for thin film heads. The CoNiFe alloy, which is used in the core of the thin film head, should have high M_s and other

* When a physically unconstrained sample is magnetized, it tends to elongate or contract. The extent to which it lengthens along the field direction between the randomly magnetized states and the saturated state is λ_s .

suitable magnetization properties such as: large permeability, μ_r , low coercivity, H_c , and small magnetostriction constant, λ_s .

1.3 Electroplating

Electrodeposited Permalloy films have been the most widely used thin film magnetic head core materials in computer mass storage. The electrodeposition of Permalloy is a low temperature process (around room temperature) capable of producing high-permeability films in the as-deposited state, without the need for heat treatment. The low equipment cost, and its suitability for use in mass production, have contributed to the success of Permalloy electrodeposition.

In plating, an electrode can have only one potential at a time, so for two or three reactions to take place simultaneously at an electrode, they must take place at the same potential. Thus, for simultaneous deposition of two or three metals in useful form, conditions must be such that the more electronegative potential of the less noble metal can be reached without the use of excessive high current density.

In the case of CoNiFe, the electrodeposition is quite feasible because the standard potentials of Fe, Co and Ni are close together (iron:-0.44 volts, nickel:-0.250 volts

and cobalt 0.277 volts). As a general rule, if the standard potential of the elements is within 200 mv of one another the codeposition would take place; otherwise, by using complexing agents the deposition potential could be brought close together.

The principal factors which affect the magnetic properties of the deposited film in any electrolytic plating process are:

- a) the composition of the bath
- b) the pH of the bath
- c) the temperature of the bath
- d) the current density
- e) the surface structure of the cathode (substrate)
- g) degree of agitation

The above factors are explored for a CoNiFe system.

In addition, a critical parameter for plating on the existing topology is compositional homogeneity across the thin film head structure, as is shown in Figure 3.

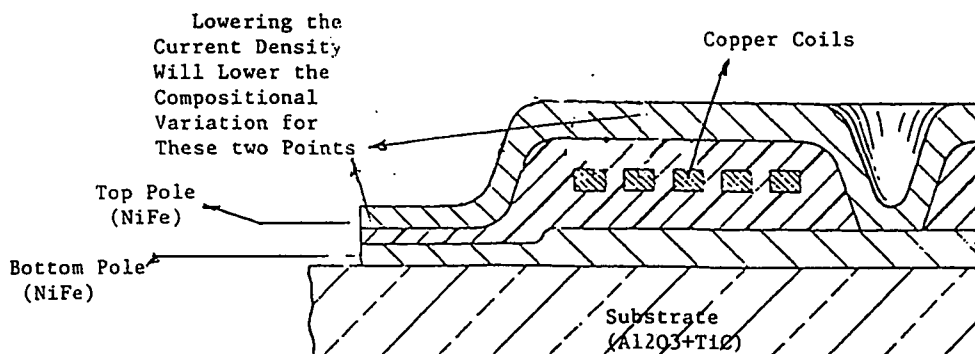


Figure 3. Sectional view of a thin film inductive head⁽⁶⁾.

It is well known that minimizing the current density minimizes this variation⁽⁶⁾. Although the lower current density has better compositional uniformity across the topology of the thin film head, it also lowers the plating rate which will lower the through-put.

1.4. Previous Work on Electrodeposition of Ternary CoNiFe Alloys

Some of the earliest work on CoNiFe alloy with very low magnetostriction was done by Tropova et al. and the results were reviewed by Srivastava⁽⁷⁾. In this work alloys with very low magnetostriction properties were deposited as 2-3 μm films onto cylindrical copper rods from baths, but the alloys were not targeted for magnetic recording and especially thin film head manufacturing. In another study⁽⁷⁾, reviewed by Srivastava, it was shown that CoNiFe obtained from Sulphamic acid baths had coercive forces of the films increasing but their saturation magnetization decreasing with increasing nickel content.

Some extensive work in this field with focus on thin film heads was done by Omata⁽⁵⁾. Omata studied the magnetic properties of CoNiFe films with high saturation magnetization prepared by evaporation and electrodeposition. The basic bath composition used is shown in Table 1.

Table 1. Basic bath composition for electrodeposition of CoNiFe⁽⁵⁾.

<u>Composition</u>	<u>Weight/liter</u>
NiSO ₄ ·6H ₂ O	240 g/l
FeSO ₄ ·7H ₂ O	98 g/l
CoSO ₄ ·7H ₂ O	16 g/l
H ₃ BO ₃	40 g/l
Saccharine Na	1.5 g/l
Na lauryl sulfate	0.25 g/l

The bath pH was around 2.4, and the bath temperature around 50 ± 2 °C. In this work, by keeping the bath condition unchanged, the various CoNiFe ternary alloys were plated by changing the current density as: $J = 4, 8, 10, 15$ and 20 mA/cm^2 . The current density versus electrodeposition composition is shown in Figure 4. Omata obtained a composition of $\text{Fe}_{45}\text{Co}_{20}\text{Ni}_{35}$ with relatively good soft magnetic properties and high B_s around 17 to 18 Kgauss, however the magnetostriction, λ_s , was positive with value of around 1.8×10^{-5} . He concluded that for obtaining a small λ_s the addition of a fourth element is necessary.

Although Omata's work was very extensive and he explored 27 different compositions, in his research he overlooked the nonmagnetostrictive composition line of the CoNiFe system as illustrated in Figure 5.

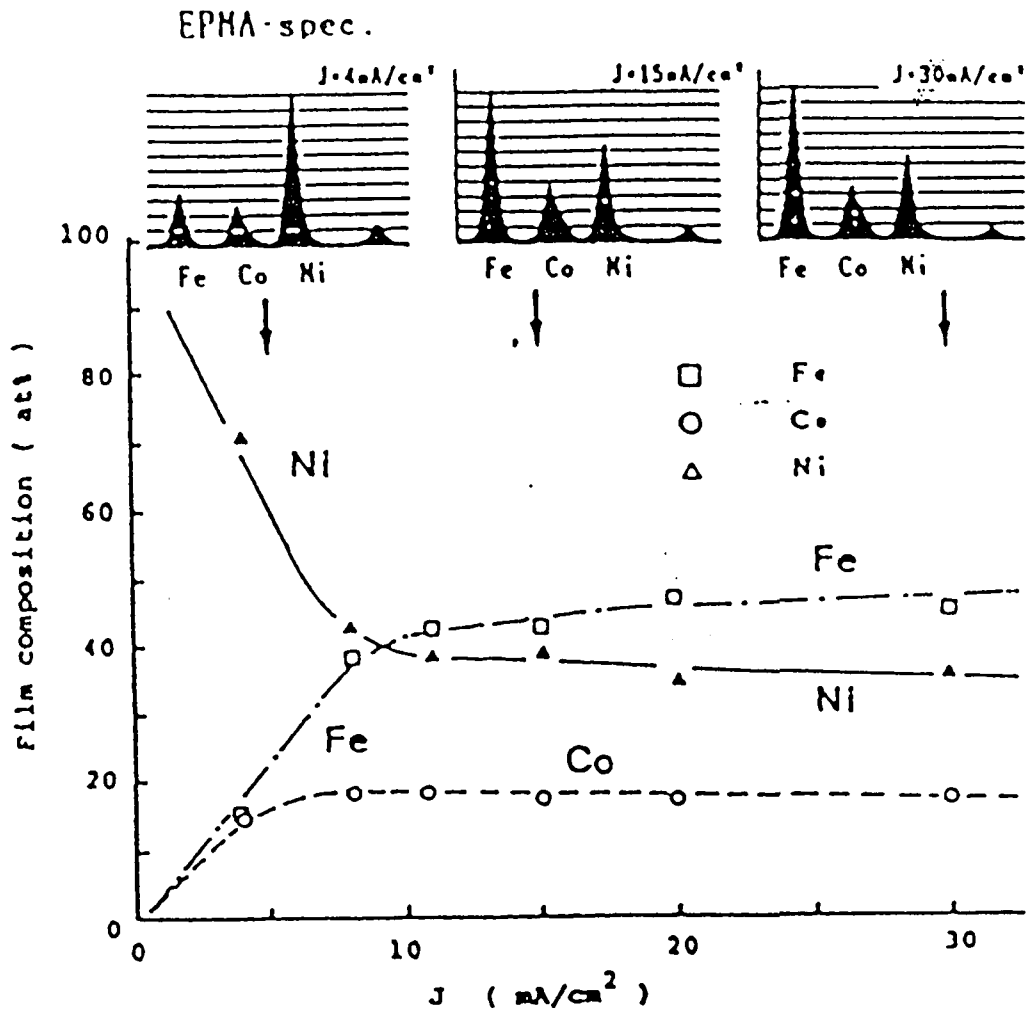


Figure 4. Current density versus film composition(5).

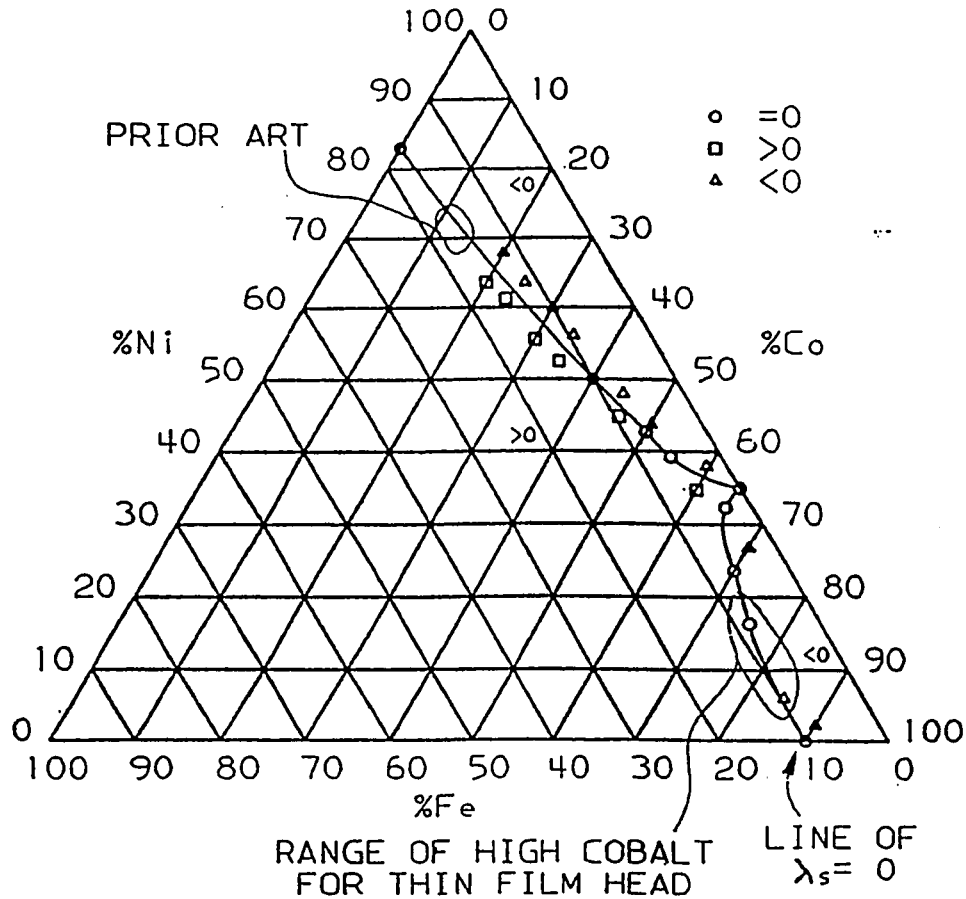


Figure 5. Non-magnetostrictive compositions of CoNiFe system⁽⁴⁾.

Anderson et al.⁽⁴⁾ used the line of non-magnetostrictive compositions of CoNiFe films which had been generated by C.H. Tolman⁽⁸⁾ and patented a series of CoNiFe alloys with small magnetostriction (λ_s) for thin film heads. A thin film head with high saturation magnetization will write well, but it is well understood that in order to be stable during the reading period the magnetostriction should be close to zero. A positive magnetostriction will not have

the desired reading characteristic. Omata's work presents the B_s , H_c , and the Curie temperature of CoNiFe-based thin films as a function of composition. This is shown in Figures 6 and 7, respectively.

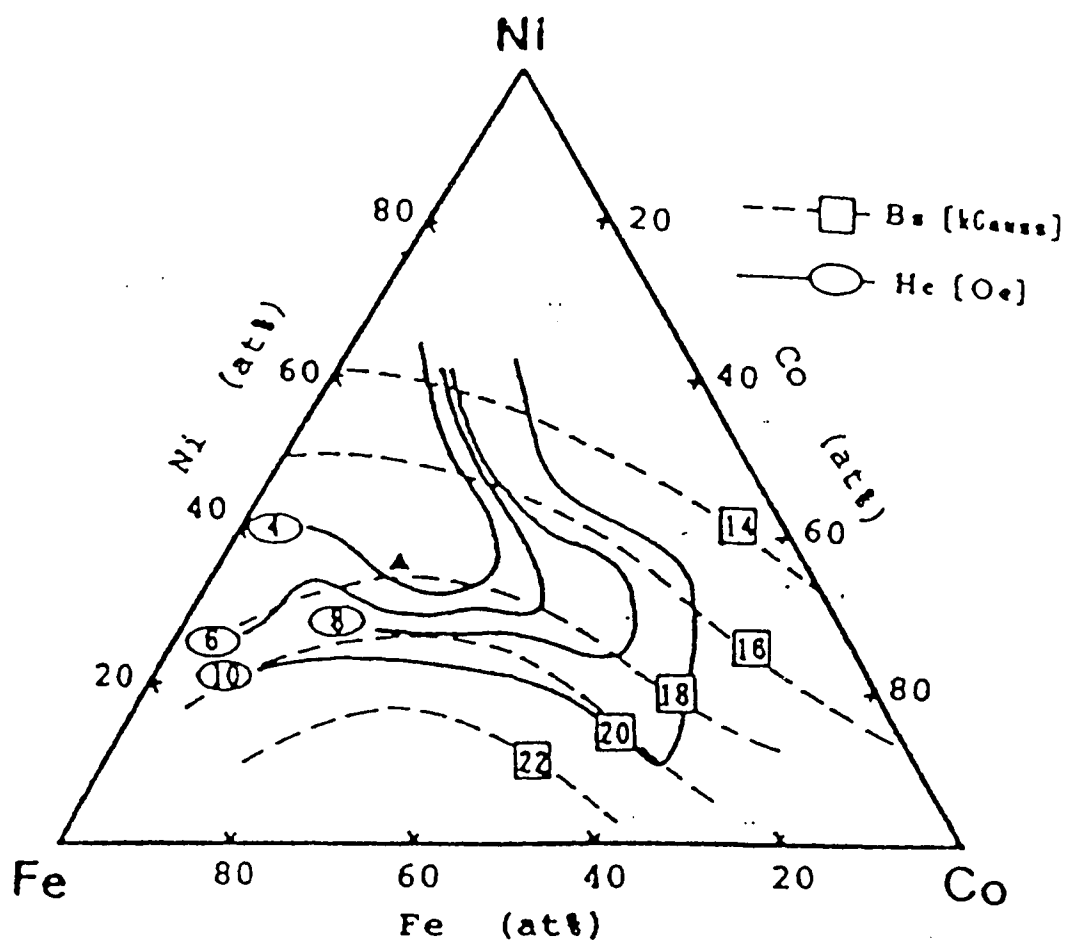


Figure 6. The B_s and H_c of CoNiFe-based thin films⁽⁵⁾.

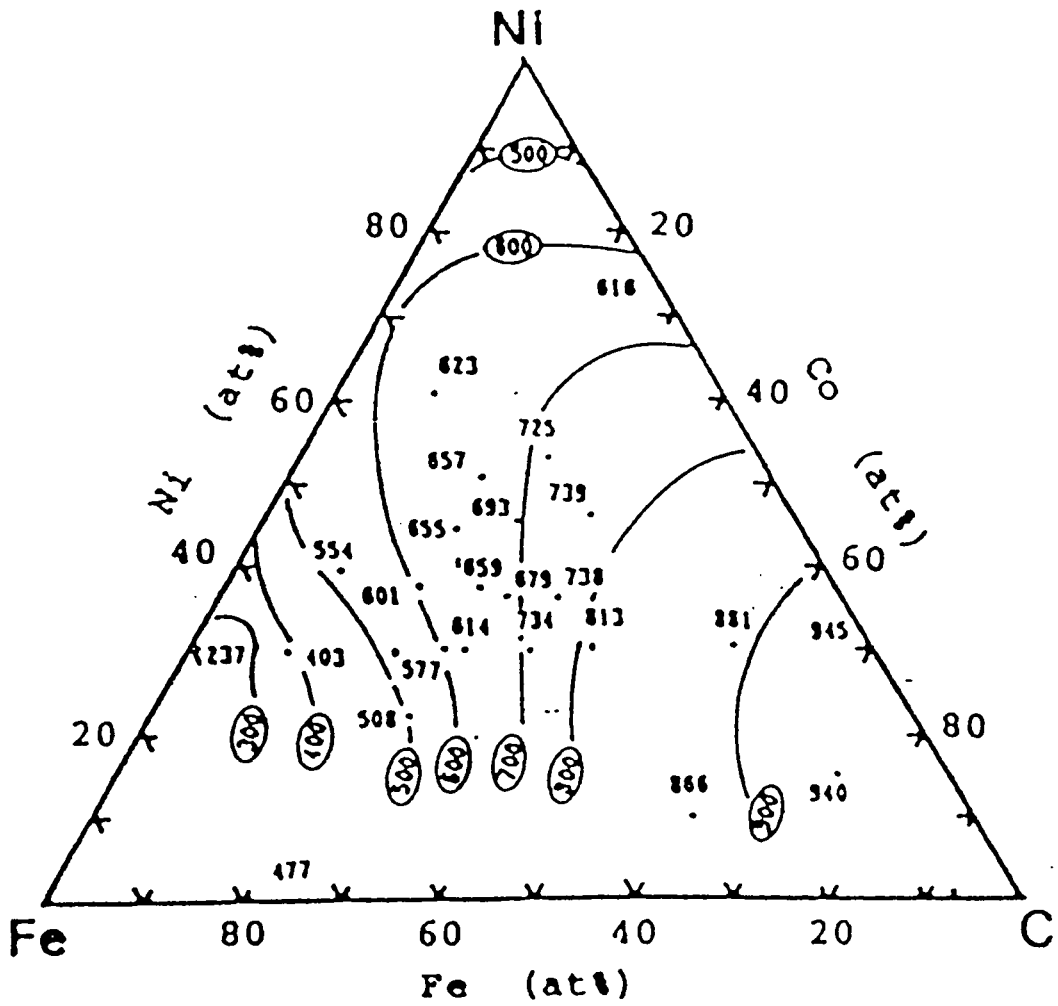


Figure 7. The Curie temperature of CoNiFe-based thin films⁽⁵⁾.

Anderson's patent⁽⁴⁾ refers to a series of prior art patents (U.S. Pat Nos 3,297,418; 3533922; 4,036,709; 4242710; and 4430171.) for CoNiFe-plated alloy with low Co concentration, and claims that a high cobalt content is required to obtain desired attributes for writing, as well as reading for thin film heads. The motivation of this patent was to come up with a new range of high cobalt in CoNiFe alloys, as shown in Figure 5. This patent discloses two different types of baths, one with low salt concentrations, and the other one with high salt bath composition depending on the current density which is being used. The specific examples of disclosed baths are presented in the Table 2.

Table 2. Examples of an electroplating low and high salt bath composition⁽⁴⁾.

Composition	Low Salt Bath (weight/Liter)	High Salt Bath (weight/Liter)
CoSO ₄ .7H ₂ O	48.0	100
NiCl ₂ .6H ₂ O	8	28
NiSO ₄ .7H ₂ O	----	13.4
FeSO ₄ .7H ₂ O	4	12
H ₃ BO ₃ .7H ₂ O	25	25
NaCl	25	25
Stress relieving Agent	1.5	1.5
Wetting Agent	0.05	0.05

Table 3. Typical properties of Co₈₀Ni₁₀Fe₁₀ plated film⁽⁴⁾.

Properties	Measured
Thickness	2μm
4πMs	16 Kgauss
H _c	1.5 Oe
H _k	10 Oe
Permeability	1600

On the basis of this patent and other previous work, it seemed logical that the focus of the thesis be around the high cobalt range of zero magnetostriction line of CoNiFe ternary diagram, as is shown in Figure 6. Besides the composition of the bath, pH, temperature and current density there are some other important factors, like agitation and circulation of the solution, which are related to the apparatus adapted for plating system. In this thesis the Read-Rite Corporation electroplating system was used to develop and optimize the bath. This is discussed in the next section.

2. EXPERIMENTAL METHODS

The experimental methods and apparatus used for the electrodeposition and characterization of CoNiFe alloy and the testing of thin films are described in this chapter. The first section is devoted to the electroplating of the thin films. The second section describes the characterization of their magnetic properties. The third section covers the experimental methods used to investigate the thin film structure and composition, and finally in the fourth section the experimental plan is detailed.

2.1. Preparation of CoNiFe Thin Film

The thin film is prepared by electrodeposition of the CoNiFe onto a glass thin wafer, which has around 1500Å sputtered NiFe seed layer. The deposited seed layer, which is on both sides of the glass substrate, has two functions. First, it makes the substrate conductive for electroplating and second, it provides a seed for growing the plated film.

2.2. Electrodeposition of CoNiFe

In electrodeposition, four basics are required: an electrolytic solution containing metal salts dissolved in solution as ions; an anode; a cathode; and a DC or pulse power supply. Plating is initiated when a DC current is

passed through the electrolytic solution. The cations are attracted toward the cathode, or negative electrode, the anions draw towards the positive electrode. The solution close to the cathode is the catholyte and that adjacent to the anode is called the anolyte. At the cathode, the reduction and simultaneous deposition of hydrogen occurs, while at the anode oxidation and evolution of oxygen take place. Since solutions of acids and bases are the best electrolytic conductors, the plating solutions are generally formulated to be either acidic or basic. Although migration of ions accounts for the overall conductivity of electrolytic solutions, usually diffusion plays a large role in bringing the ions to be discharged to the face of the cathode, which is the substrate. The number of grams of the deposited metal at the cathode is calculated from Faraday's law⁽⁹⁾ and for 100% plating efficiency one can write:

$$G = I e t / 96500 \quad (2.1)$$

where I is the current in amps, e the electrochemical equivalent weight* in grams and t the time in seconds.

In binary alloy plating the electrochemical equivalent of the alloy is calculated as following:

* The electrochemical equivalent weight of an element or compound is its atomic (or molecular) weight divided by the valence change or number of electrons involved in the reaction

$$e_a = e_1 e_2 / (f_2 e_1 + f_1 e_2) \quad (2.2)$$

where e_a is the electrochemical equivalent of the alloy, e_1 and e_2 are the electrochemical equivalents of the two metals, f_1 and f_2 are the fractions by mass of the respective metals in the alloy; $f_1 + f_2 = 1$. This calculation for ternary plating becomes rather complicated; however, for big variations in composition the change of e is fairly small and usually can be neglected. By assuming that the amount of e remains constant and the efficiency of the plating is close to 100%, one can keep the amount of deposited metal constant by :

$$I \times t = \text{Constant} \quad (2.3)$$

Based on this, at different current densities the different plating times can be calculated in such a way that the amount of deposit and consequently the thickness of the plated film remains constant.

In alloy plating two conditions must be met:

- 1) at least one of the metals must be deposited independently.

2) their deposition potentials, or the standard potential in the table of electromotive force, must be fairly close or should be brought close together by complexing.

In alloy plating an electrode can have only one potential at a time and for two or more reactions to take place at the same time they should happen at the same potential. By considering the Nernst Equation:

$$E = E^{\circ} + (RT/nF) \ln a + P \quad (2.4)$$

where P is the polarization or departure from equilibrium conditions due to diffusion limited transport, for alloy plating two different cathodic process should occur simultaneously:

$$E_1^{\circ} + (RT/nF) \ln a_1 + P_1 \cong E_2^{\circ} + (RT/nF) \ln a_2 + P_1 \quad (2.5)$$

where E° is a constant characteristic of the metal electrode, R the gas constant ($8.314 \text{ J K}^{-1} \text{ mole}^{-1}$), T the absolute temperature, n the valence change (number of electrons taking part in the reaction), F the Faraday's constant, a the activity of metal ions.

Since P_1 and P_2 cannot be vastly different, for alloy plating to take place either E_1° and E_2° , i.e. the standard

potentials, must already be close together or the activities should be adjusted by means of complexing agents to make the equation valid. As a general guide, if the standard potentials, in the table of electromotive force series, are within 200 mV of each other the codeposition should take place. The electromotive force series is shown in Table 4.

Table 4. The electromotive force(emf) series⁽⁹⁾.

Electrode	Potential (V)	Electrode	Potential (V)
Li = Li ⁺	-3.045	Co = Co ²⁺	-0.277
Rb = Rb ⁺	-2.93	Ni = Ni ²⁺	-0.250
K = K ⁺	-2.924	Sn = Sn ²⁺	-0.136
Ba = Ba ²⁺	-2.90	Pb = Pb ²⁺	-0.126
Sr = Sr ²⁺	-2.90	Fe = Fe ²⁺	-0.04
Ca = Ca ²⁺	-2.87	Pt/H ₂ = H ⁺	0.0000
Na = Na ⁺	-2.715	Sb = Sb ³⁺	+0.15
Mg = Mg ²⁺	-2.37	Bi = Bi ³⁺	+0.2
Al = Al ³⁺	-1.67	As = As ³⁺	+0.3
Mn = Mn ²⁺	-1.18	Cu = Cu ²⁺	+0.34
Zn = Zn ⁺	-0.762	Pt/OH = O ₂	+0.40
Cr = Cr ³⁺	-0.74	Cu = Cu ⁺	+0.52
Cr = Cr ²⁺	-0.56	Hg = Hg ₂ ²⁺	+0.789
Fe = Fe ²⁺	-0.441	Ag = Ag ⁺	+0.799
Cd = Cd ²⁺	-0.402	Pd = Pd ²⁺	+0.987
In = In ³⁺	-0.34	Au = Au ³⁺	+1.50
Pb = Pb ⁺	-0.336	Au = Au ⁺	+1.68

As can be seen, the standard electrode potential of Fe, Ni and Co are 191 mV apart which indicates that they can be plated satisfactorily from the same type of solution without requirement of complexing agents.

The metal content of alloy plating baths must be replenished, usually by anodic solution. If one constituent of the alloy is a relatively minor one, the main constituent may be used as an anode and the minor one is replenished chemically.

As was described before, the variables that can be controlled in alloy plating are: composition of the bath, pH, temperature, current density, and agitation. These factors require stringent control because a change in one of them will affect one of the constituents of the alloy more than the other and thus change the composition of the deposit. How these variables will affect the deposit should be determined empirically; however, in CoNiFe plating the following can be used as a guideline.

An increase in current density will increase the proportion of the less noble metal, in this case Fe. From a theoretical point of view, Ni-Fe and by the same token CoNiFe alloy plating is interesting because it exhibits anomalous codeposition; that is, the less noble metal, Fe, deposits preferentially to the more noble metal. For instance, where the ratio of Ni^{++}/Fe^{++} in solution of different Permalloy baths varies from 30:1 to about 70:1, the ratio in the plated film is about 4.3:1⁽⁶⁾. The less noble metal, Fe, appears at unexpectedly high concentration in the deposit. Among the several explanations, the one

which is most consistent with the observations is the model of Dahms and Croll⁽¹⁰⁾. They note that H₂ evolution during deposition will cause a local pH rise near the electrode surface, which causes the precipitation of Fe(OH)₂ in the vicinity of the electrode surface. Such hydroxide precipitation has been known⁽¹⁰⁾ to impede the discharge of other metal ions, and thus suppresses the deposition of Ni but permits a high discharge rate of Fe²⁺.

In another report the effect of temperature and pH has been studied on anomalous codeposition of Ni-Fe⁽¹⁰⁾ based on the claim that the deposition of Ni-Fe alloy proceeds with simultaneous Ni²⁺ discharge under activation control, Fe²⁺ discharge under mass transport, and H₂ evolution under mass transport control. This will explain the role of agitation in the bath. In some experiments which were done by the author it was noticed that without the agitation the amount of Ni in the deposited film would increase, which is an indication of different discharging mechanisms for Ni²⁺ and Fe²⁺ ions.

A schematic diagram of a plating station is shown in Figure 8. The cell is designed for plating 4" square wafers.

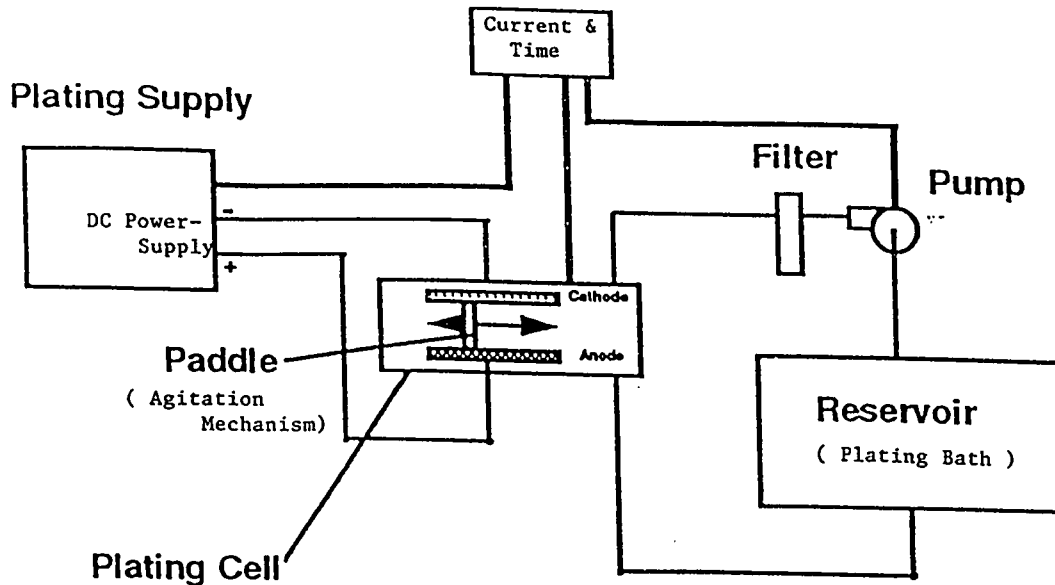


Figure 8 Schematic Diagram of plating station⁽¹¹⁾.

2.3. Magnetic Characterization of Plated Thin Films

Among the most important magnetic properties of the thin film for magnetic recording heads are: saturation magnetization ($4\pi M_s$), coercivity (H_C), anisotropy (H_k), saturation magnetostriction coefficient (λ_s) anisotropy dispersion (α_{90}) and permeability (μ), as mentioned in the previous chapter. These parameters are measured by a M-H loop tracer.

2.3.1. MH and BH loops

A typical MH curve for soft magnetic material, with uniaxial anisotropy and low coercive force is shown in Figure 9⁽¹²⁾ and the BH loop curve for a typical thin film head material is presented in Figure 10 (since $B - H = 4\pi M$, a

BH curve for a soft ferromagnetic material, where $B \gg H$, will differ from an MH curve only by a factor of 4π applied to the ordinate).

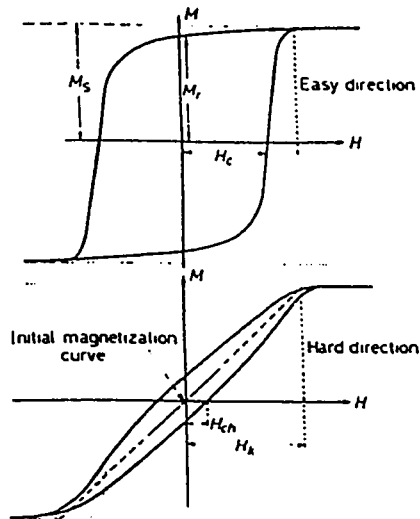


Figure 9. Typical easy and hard direction hysteresis loops of an anisotropic film⁽¹²⁾.

In Figure 9 the following notation is used:

- (i) H_c is the coercivity in the easy direction.
- (ii) The hard direction hysteresis loop has coercivity H_{ch} .
- (iii) H_k is the anisotropy field. It is the field required to rotate the magnetization coherently from the easy to the hard direction against a uniaxial anisotropy. In this case H_k is given by : $H_k = 2K/M_S$ for a film with uniaxial anisotropy constant K and magnetization M_S .
- (iv) The easy direction remanence is M_r .

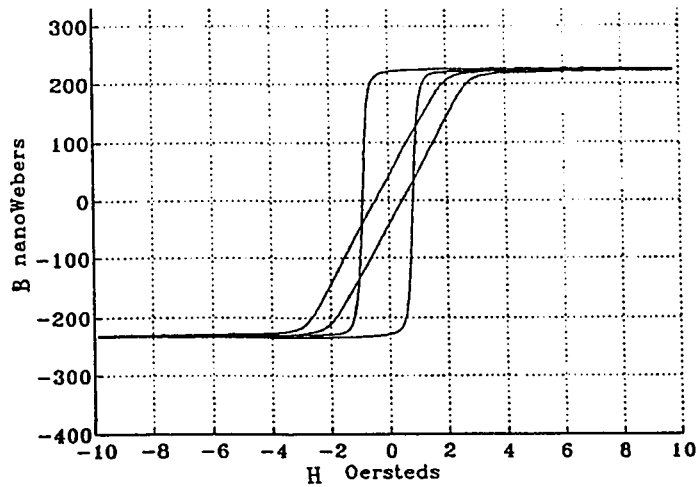


Figure 10. Typical B-H loop of plated NiFe film.
(courtesy of Read-Rite)

2.3.2. Magnetic Units

Although M , the magnetization, is the variable which most clearly describes the magnetic state of a specimen, many phenomena are best described in terms of the magnetic flux density, B . The relationship between B , H , and M is expressed differently in the two most common systems of units. In this report and from now on the MKSA system will be used with the older cgs-emu system in parenthesis. The defining relationship is:

$$B = \mu_0 (H + M) \quad \{ B = H + 4\pi M \} \quad (2.6)$$

where $\mu_0 = 4\pi 10^{-7}$ henry/meter is the permeability in free space and B is expressed in weber/meter². B can also be expressed in gauss. The gauss (10^{-4} Weber/m²) is most

typically used in industry. The MKSA unit for H and M is the ampere/meter. The cgs unit for H is the oersted. The unit of $4\pi M$ in the cgs system is gauss.

2.3.3. Requirement of Thin Film Head Material

The main requirements for the desired head, which contains a film of soft magnetic material, are high saturation magnetization, M_s (because the head, which acts as a transducer must provide an intense magnetic field at the surface of the medium to write the digital transition), large permeability (easily magnetized) over a wide frequency range, low coercivity (H_c represents the field necessary to reduce the magnetization to zero), small saturation magnetostriction constant, λ_s (to minimize the magnetic misbehavior of the material under stress) and good thermal stability within -20°C to 85°C temperature range.

2.3.4. M-H Loop Tracer

A hysteresis loop tracer, SHB instrument model 108, is shown schematically in Figure 11.

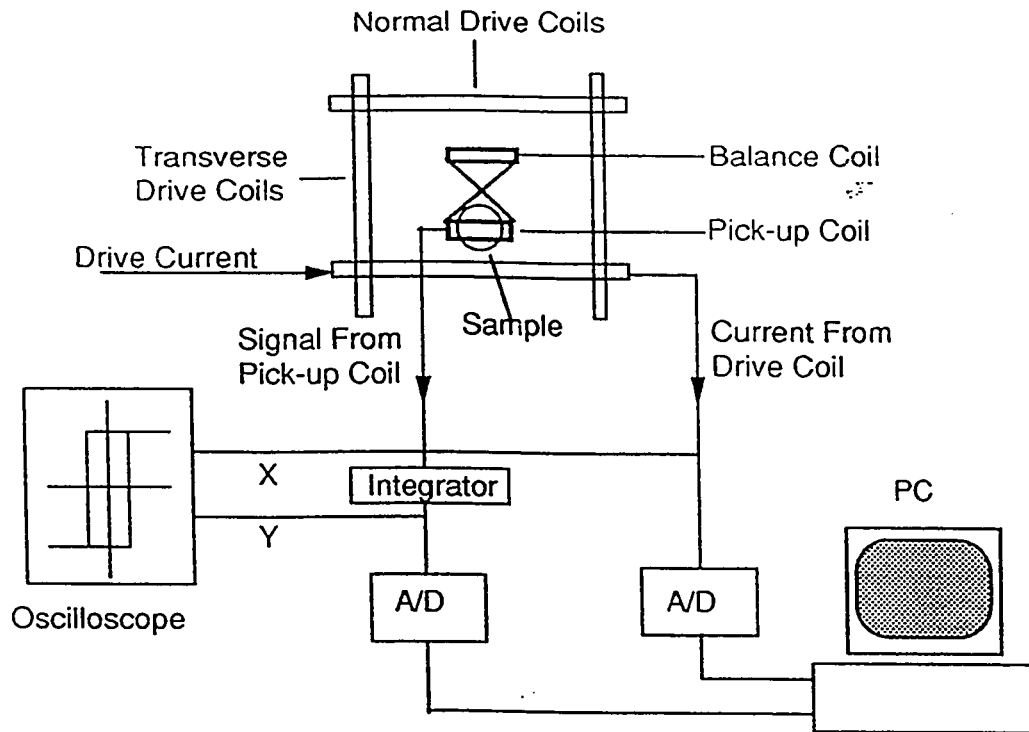


Figure 11 Schematic Diagram of M-H loop tracer⁽³⁾.

The instrument has three components: a pair of Helmholtz coils, which produce drive field; a pick-up coil, which surrounds the sample and measures the moment of the sample; and finally the oscilloscope. The compensated pickup voltage, after integration and amplification, is fed to the vertical plane of the oscilloscope so that a hysteresis loop is generated. The data from oscilloscope is then digitized into a PC and consequently displayed on a computer screen. The M_s value printed out by the loop tracer is not the real magnetic moment, but the magnetic flux through the sense coil. A calibration factor based on thickness needs to be

used to calculate the actual magnetic moment of the sample according to the following formula:

$$M_s = B_s(nw) / 114.808 \times t \text{ (Cm)} \quad (2.7)$$

Coercivity, H_c , and anisotropy, H_k , is measured by MH tracer directly and the saturation magnetization constant, λ_s , is measured indirectly. When a sample film deposited on a glass test wafer is under a known stress, its anisotropy (H_k) changes. This change in H_k is related to saturation magnetostriction coefficient, λ_s , by:

$$\lambda_s = M_s \Delta H_k / 3 \sigma \quad (2.8)$$

where M_s is saturation magnetization, ΔH_k is the change in anisotropy and σ is the applied stress. Since the calculation of the stress (σ) can not be done accurately, the calculation of λ_s is not possible. However, it can be assumed that the stress is constant because the fixture, which is used to bend the wafer, is applying the same stress all the time, and the substrate thickness is also the same. By using the constant stress assumption, the λ_s of CoNiFe can be related to the λ_s of NiFe by the following equation:

$$\lambda_{s\text{CoNiFe}} / \lambda_{s\text{NiFe}} = (M_{s\text{CoNiFe}} / M_{s\text{NiFe}}) (\Delta H_{k\text{CoNiFe}} / \Delta H_{k\text{NiFe}}) \quad (2.9)$$

2.4. Film Thickness, Composition, and Structural Analysis

2.4.1. Thickness Measurement

For thickness measurements a special mask was used to lay down five 1 mm diameter circles of photoresist on the center of the wafer and on the center of each quadrant, as shown in Figure 12.

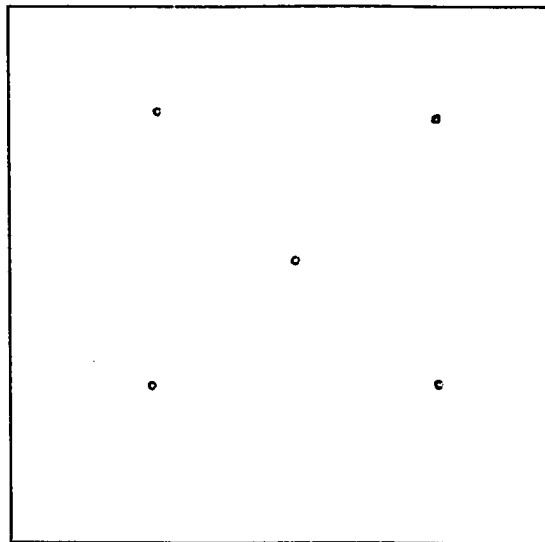


Figure 12. Photoresist mask layout for thickness measurement.

After plating the glass test wafer, the photoresist was stripped and the thickness of the plated film was measured with a Dektak profilometer.

2.4.2. Energy Dispersive X-ray Microanalysis (EDX)

The analyses of the samples were done by Energy Dispersive X-ray Microanalysis (EDX). The EDX microanalysis is one of the easiest and best methods for analyzing thin film samples. The technique is practically nondestructive and requires no sample preparation. In EDX microanalysis, electrons of appropriate energy impinge on a sample and cause the emission of X-rays whose energies and relative abundance depend upon the composition of the sample.

Components of a typical energy dispersive microanalysis system are shown in Figure 13.

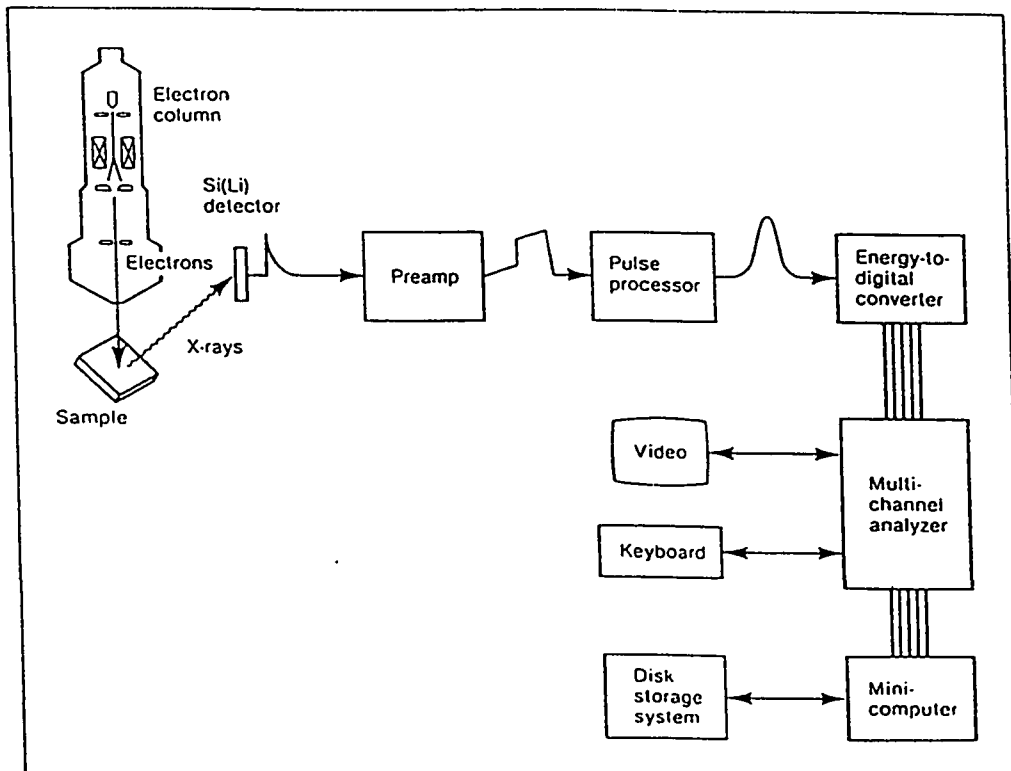


Figure 13. Components of a typical EDX system⁽¹³⁾.

2.4.3. X-Ray Diffractometer

The X-ray diffraction technique is used to identify the structure of the sample. X-ray diffraction is an extremely powerful tool in the study of internal structure of materials. The technique works on the basis of the Bragg equation which describes the condition for constructive interference for X-ray scattering from atomic planes of a crystal⁽¹⁴⁾:

$$2d \sin \theta = n\lambda \quad (2.10)$$

where d is the distance between the planes of the crystal, θ is the diffraction angle, and λ is the wavelength of the incident radiation. Diffraction occurs from crystallites which happen to be oriented at the angle to satisfy the Bragg condition. From the diffraction pattern, crystal structure of the material can be determined.

2.5. Experimental Procedure

2.5.1. Plating Station

The Read-Rite Corporation plating setup was used to develop the bath. The schematic diagram of the station was shown previously in Figure 8. The station consists of one cell with reciprocal paddle movement designed for 4 inch square wafers.

2.5.2. Bath Makeup and Chemistry

First, deionized (DI) water was used to determine the minimum bath level to achieve effective circulation. This turned out to be 60 liters. Once the volume was determined, the bath was made up to achieve the composition shown in Table 5. This bath composition was chosen according to the Anderson's patent discussed in Section 1.4.

Table 5. Bath makeup and chemistry.

<u>Composition</u>	<u>weight (g/l)</u>	<u>Conc. of</u> <u>Dischargeable Ions</u> <u>(g/l)</u>
CoSO ₄ ·7H ₂ O	100	Co ⁺⁺ 20.97
NiCl ₂ ·6H ₂ O	28	Ni ⁺⁺ 6.92
NiSO ₄ ·7H ₂ O	13.4	Ni ⁺⁺ 2.80
FeSO ₄ ·7H ₂ O	12.8	Fe ⁺⁺ 2.41
H ₃ BO ₃ ·7H ₂ O	25	
NaCl	25	
Na-Saccharin	1.5	
Wetting Agent	0.05	

After the bath makeup, the bath was analyzed, by using the chem-lab facility in Read-Rite, to ensure that the desired chemical composition had been achieved.

2.5.3. Bath Designs

The design of the bath and the experiments were done in two Phases. In Phase I, by varying the current density, the film composition resulting in the best properties was determined. In Phase II, the current density was kept at 3 mA/cm² while the bath composition was varied until the desired film composition, determined in Phase I, was achieved.

Phase I

The operating parameters for the plating bath were:
pH = 3.0, RPM of the paddle = 40, which is the maximum without splashing the solution out, and the temperature = 30.0 ± 0.3 °C. These are close to the current setups for NiFe plating in Read-Rite Corporation. They were chosen, based on the following considerations⁽⁴⁾, to achieve acceptable plating.

pH: Can be in the range of 2.5 to 3.5.

Temperature: 25 to 35 °C.

Paddle Speed in revolution per minute(RPM): The faster the better. The faster the paddle agitation, the thinner the diffusion layer. The diffusion layer is the layer close to the cathode with different composition than the bulk solution. As was mentioned before, the diffusion layer plays a large role in bringing the dischargable ions to the

face of the cathode (substrate). The thinner the diffusion layer is, the better ions can be replenished and discharged from bulk solution.

The desirable composition range for the plated film is shown in Figure 14.

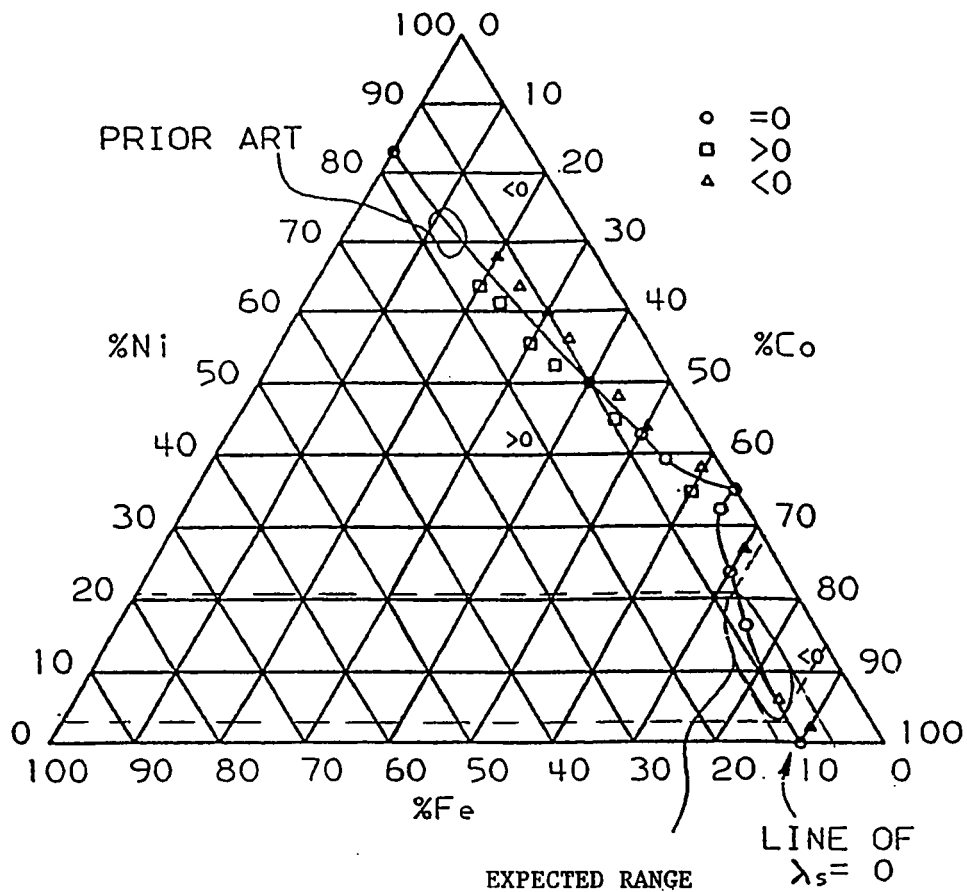


Figure 14. Expected composition range for the plated film⁽⁴⁾.

Based on the discussion of patent results in Section 1.4, the desired film composition must be in the range of $\text{Co}_{72-87} \text{Ni}_{3-21} \text{Fe}_{6-13}$. However, the ratio in the plating bath is : Co:Ni:Fe : 63:30:7. In order to change the plated film composition to study a series of plated films with different compositions, either the bath chemistry needs to be changed or the current density. Since changing the bath chemistry is very cumbersome and time consuming the alternative was chosen.

Phase II

A 3 mA/cm² current density was used, since prior results show that the composition gradient across the topology of the thin film structure is minimum at this current density and an acceptable plating efficiency is maintained.

Modifying the bath was done by small additions of $\text{CoSO}_4 \cdot 7\text{H}_2\text{O}$ and $\text{FeSO}_4 \cdot 7\text{H}_2\text{O}$ to the bath at a time and running the test wafer at 3 mA/cm² to achieve the desired composition, thickness and magnetic properties. The final acceptable sample was sent out for X-ray Diffractometry to determine crystal structure.

Figure 15 shows a flow chart, which represents the methodology of Phase II of the experiment.

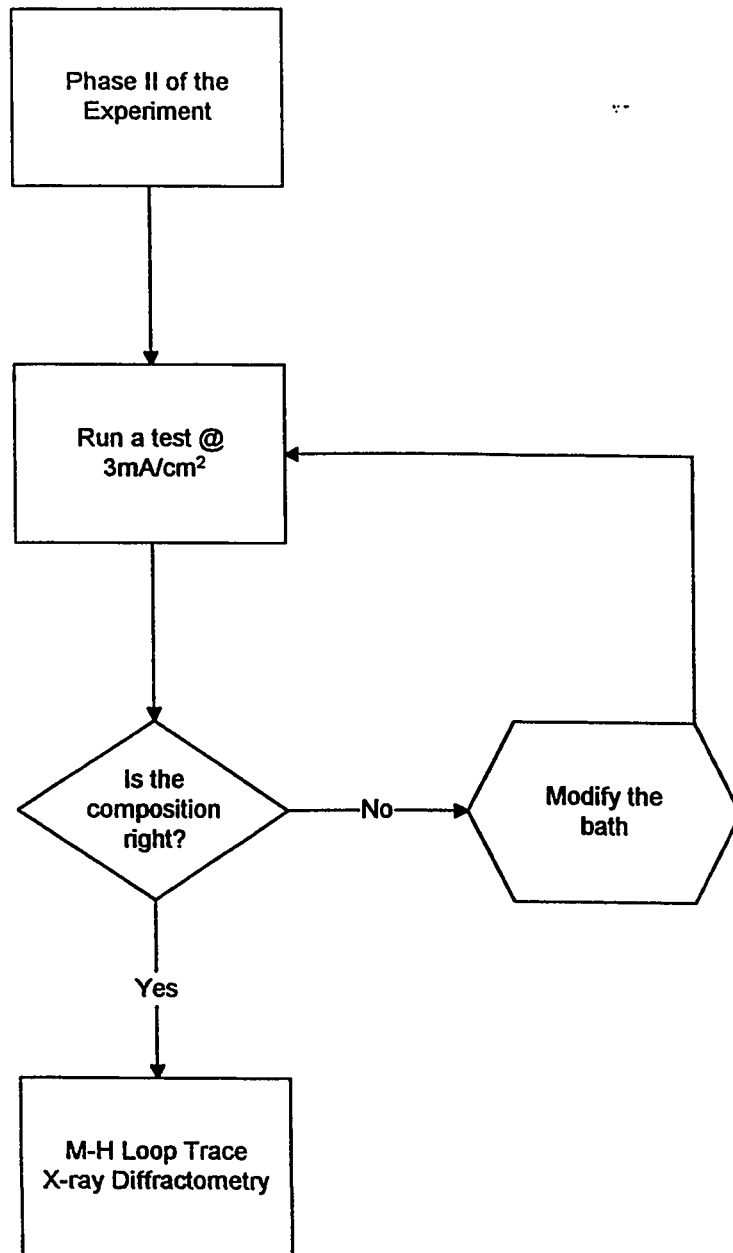


Figure 15. Flowchart representing the methodology of Phase II.

3. RESULTS AND DISCUSSION

3.1. Bath Control

CoNiFe plating, just like any other electrolytic plating process, requires stringent control of the operating parameters. The operating parameters for the plating bath, as was mentioned in the experimental procedure section, are: temperature, pH, agitation, and chemistry of the bath. In this section the mechanism of controlling the operating parameters is discussed.

3.1.1. Temperature

To maintain the temperature of the plating cell within the range specified, for CoNiFe plating, i.e., 30 ± 0.3 °C, a heat exchanger unit is used in the bath. Polyethylene heat exchange coils line the inside of the reservoir and are connected to a temperature controller unit. The unit heats up the bath or removes the heat, based on the signal input from a thermometer inside the plating cell. The trend chart for the variation of temperature for some of the plated test wafers is shown in Figure 16. Temperatures were recorded at the beginning and end of the plating cycle. As can be seen, the variation of the temperature is well within the specified range.

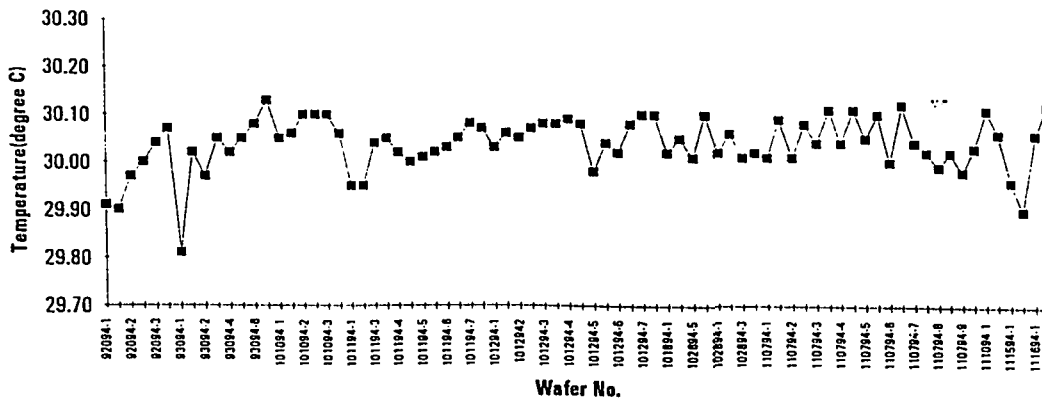


Figure 16. Temperature variation of the bath for the plated test wafers.

3.1.2. pH

In order to monitor the pH of the bath and maintain it within the specified range, i.e: 3.0 ± 0.5 , an on-line pH meter was used. The pH meter consists of a pH/reference electrode assembly, fitted to the end of the hermetically sealed tube, which protrudes downward from the top of the tank into the plating bath. A digital microprocessor-based pH controller displayed the bath pH continuously. The controller is capable of resolution and accuracy of ± 0.01 pH unit. To ensure that the pH readings were accurate, a sample of the solution was taken and the pH was checked with an outside calibrated pH-meter on a daily basis. Figure 17 shows the trend chart of pH variation during plating of some of the wafers.

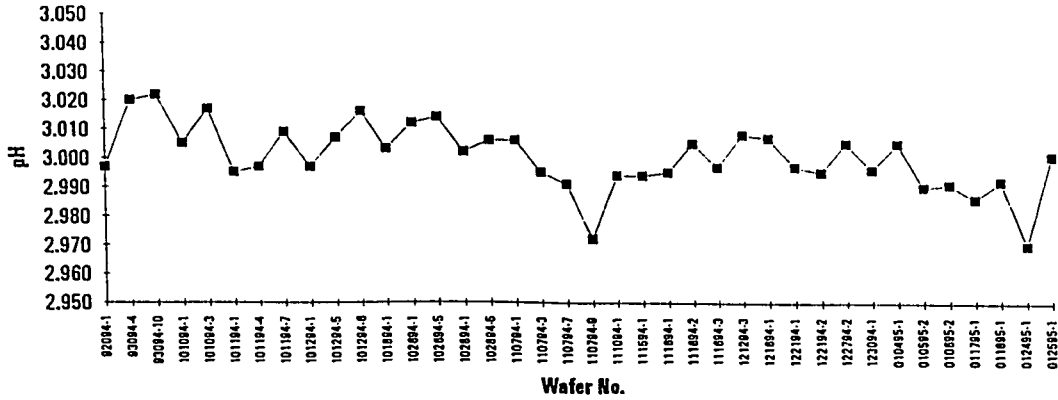


Figure 17. pH variation of the bath during plating some of the test wafers.

3.1.3. Bath Chemistry

To control the bath chemistry, the bath was analyzed twice a week for Co, Ni, and Fe⁺⁺ determination. The analysis of the bath was done by using the inductively coupled plasma-atomic emission spectrometry(ICP-AES). The working principle of ICP-AES is like the other atomic emission spectroscopy, where the sample is subjected to very high temperature. The temperature is high enough to cause not only dissociation of the sample into atoms but to cause significant amount of collisional excitation(and ionization) of the sample atoms. Once the atoms or ions are in their

excited states, they can decay to lower states through thermal or radiative(emission) energy transitions. In AES, the intensity of the light emitted at specific wavelengths is measured and used to determine the concentrations of the elements of interest. In ICP-AES, argon-supported inductively coupled plasma is used as a source for electrical discharge which in terms acts as a thermal source to dissociate sample molecules into free atoms⁽¹⁵⁾. Figure 18 presents the analyses data for Co, Ni, and Fe⁺⁺ in the course of the experiments.

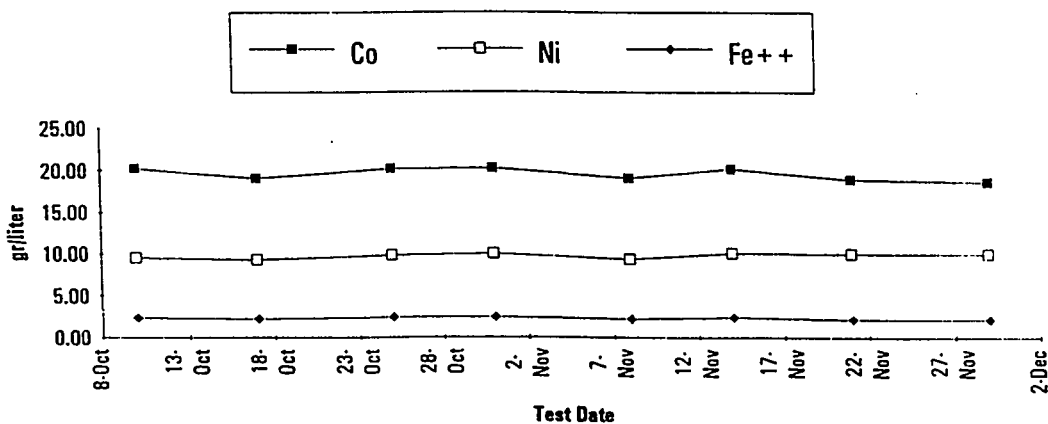


Figure 18. Chemical analyses data.

Constant composition of the plated alloy requires unchanging Co, Ni, Fe, and pH in the plating bath. During plating Co, Ni, and Fe⁺⁺ are consumed and the pH will rise due to H₂ discharge at cathode. The consuming rate depends on the plating current density. In order to maintain constant bath concentrations of these substances in the process, the plating solution is automatically replenished with an automatic add-back system. The add-back system contains hydrochloric acid, cobalt sulfate heptahydrate, and iron sulfate heptahydrate, and deionized (DI) water. The replenishment of Ni is done by the Ni-anode. Based on the following calculations a solution containing 3.25 ml of HCl, 25.5 g of CoSO₄·7H₂O, 2.94 g of FeSO₄·7H₂O per one liter of deionized (DI) water was prepared and metered into the bath at the rate of 1 cc/min during the plating cycle.

By assuming a film composition of Co₈₀Ni₁₀Fe₁₀ and a measured plating rate of 7.8434 X 10⁻⁶ cm/min, the amount of depleted Co and Fe in g/min was calculated, as follows:

$$\begin{aligned} \text{Co(g/min)} &= 7.8434 \times 10^{-6} \times 95.75 \times 8.9 \times 0.8 \\ &= 5.35 \times 10^{-3} \end{aligned}$$

$$\begin{aligned} \text{Fe(g/min)} &= 7.8434 \times 10^{-6} \times 95.75 \times 7.86 \times 0.1 \\ &= 5.91 \times 10^{-4} \end{aligned}$$

where 95.75 is the area of the plated test wafer in cm^2 , 8.9 is density of Co in g/cm^3 , and 7.86 is the density for Fe in g/cm^3 .

The calculated amounts correspond to addition of 2.55×10^{-2} g/min of $\text{CoSO}_4 \cdot 7\text{H}_2\text{O}$ and 2.94×10^{-3} g/min of $\text{FeSO}_4 \cdot 7\text{H}_2\text{O}$. The amount of the addition of the HCl to the addback solution was based on the author's experience with the behavior of NiFe bath and assuming the similarity between that and the current CoNiFe bath, regarding the pH variation, during plating.

3.1.4. Specific Gravity

In the course of the experiments, it was noticed that the bath becomes concentrated and its volume decreased because of evaporation. Although the proportion of deionized (DI) water used in the formulation of add-back solution was increased to the maximum amount, the automatic add-back system was incapable of compensation of the evaporative loss of bath volume. It was decided to monitor the specific gravity of the bath on a daily basis, and keep it constant by addition of deionized (DI) water to the bath. The specific gravity of the bath was measured by using a specific gravity hydrometer.

3.1.5. Agitation

The 60 liter reservoir supplies fresh filtered plating solution to a paddle-cell continuously. The plating cell is equipped with 0.05 hp magnetically coupled centrifugal pumps and submicron filter assembly. Solution enters the pump from an outlet near the bottom of the reservoir. Schematic diagram of the plating station was shown in Figure 10 previously. Agitation in the cell is controlled by a paddle. As was mentioned before, paddle speed is monitored in revolutions per minute(RPM). The higher RPM, the thinner the diffusion layer which brings the dischargable ions to the face of cathode(wafer). The thinner the diffusion layer is, the better ions can be replenished and discharged from bulk solution. The RPM of the paddle was selected to be 40, which is the maximum without splashing the solution out. Paddle speed is monitored on a meter with accuracy of ± 0.2 RPM.

3.2. Evaluation of the Plated Film

Compositional analysis, magnetic properties, thickness, roughness, and hardness of the plated films were the properties that were evaluated. In this section the characterization of the plated CoNiFe film will be discussed.

As was discussed before, the first set of experiments was run to determine the current density which produced the desired plated film composition. A series of glass test wafers, seeded with NiFe seed, layer and masked with the pattern shown in Figure 12 was run at seven different current densities. Table 6 shows the experimental test and measurement matrix for the set of experiments.

Table 6. Experimental test and measurement matrix.

Current Density (mA/cm ²)	Magnetic properties (MH-Looper)	Composition (EDX)	Thickness (Dektak)
3	X	X	X
4	X	X	X
5	X	X	X
6	X	X	X
7	X	X	X
8	X	X	X
9	X	X	X
11	X	X	X
13	X	X	X
15	X	X	X
20	X	X	X
30	X	X	X

To obtain multiple points for each measurement, three test wafers were run at each current density.

The thickness target for the samples was $2.0 \pm 0.2 \mu\text{m}$. The specification range for the thickness target was chosen based on the current uniformity data across the 4 inch wafer for NiFe plating.

After measuring the film composition and magnetic properties, the optimum film composition was selected based on the highest saturation magnetization, $4\pi M_s$, zero magnetostriction constant, λ_s , low coercivity, H_c , and low anisotropy field, H_k .

3.2.1. EDX Measurements of the Film Composition

The EDX system was calibrated with the FeNiCo NIST(National Institute of Standard & Technology) Standard reference material sample, and then the repeatability of the measurements was checked by measuring the standard for 10 consecutive times. In Table 7 the measurement data for repeatability test is presented.

Table 7. NiFeCo NIST-Standard Measured on the EDX.

Test No.	Fe Wt.%	Ni Wt.%	Co Wt.%	Nb Wt.%	Ti Wt.%	Al Wt.%
1	40.95	38.50	16.62	2.03	1.47	0.43
2	41.34	37.83	16.87	2.08	1.38	0.51
3	41.30	37.61	16.75	2.03	1.37	0.98
4	40.72	38.55	16.54	2.19	1.49	0.49
5	41.11	38.13	16.89	2.00	1.42	0.46
6	41.16	37.99	16.94	2.10	1.39	0.42
7	41.80	37.59	16.82	1.95	1.39	0.45
8	41.52	37.66	16.87	2.05	1.47	0.43
9	41.59	37.89	16.83	1.96	1.30	0.43
10	41.85	37.75	16.59	1.98	1.37	0.45
Mean	41.33	37.95	16.77	2.04	1.41	0.50
Std. dev.	0.36	0.35	0.14	0.07	0.06	0.15
Nominal	40.50	37.78	16.10	2.99	1.48	0.99

Based on the results, the standard deviation of the EDX measurements are: 0.36 wt.% for Fe, 0.35 wt.% for Ni, and 0.14 wt.% for Co.

3.2.2. MH loop Measurements of the Plated Film

The magnetic properties of the plated films were measured on a SHB instrument model 108 M-H loop tracer. The schematic diagram of the M-H loop tracer and its components were presented in Figure 11 (previous chapter). A MH loop

of a typical CoNiFe plated film along with a MH loop of NiFe plated film, which is the current material used for the core of the thin film head, are presented in the Figure 19.

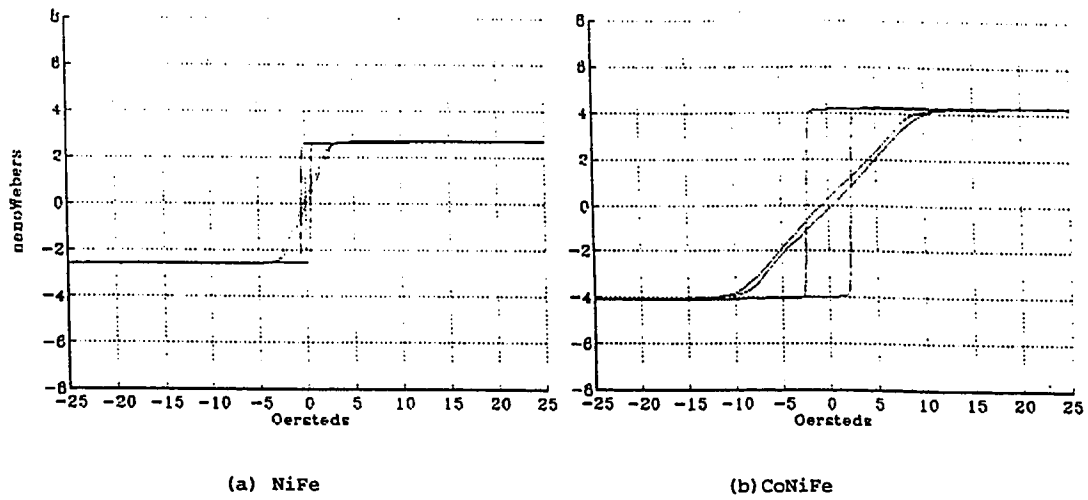


Figure 19. Typical MH loop traces for Plated (a) NiFe and (b) CoNiFe (Courtesy of READ-RITE).

In a simple study to measure the repeatability of the MH loop tracer one of the samples were measured five times. The data are presented in Table 8.

Table 8. Repeatability study of the M-H loop tracer.

Measurements	No.1	No.2	No.3	No.4	NO.5	Std.Dev.
B_{sh} (nW)	419.7	419.8	412.3	419.6	419.4	3.28
H_{kh} (Oe)	11.58	11.53	11.38	11.44	11.58	0.09
ΔH_k (Oe)	0.83	1.01	1.01	0.94	0.81	0.10
H_{ch} (Oe)	0.6506	0.6671	0.6475	0.6046	0.6761	0.03
B_{se} (nW)	419.3	418.9	411.7	419.0	419.0	3.29
B_{re} (nW)	408.4	408.2	408.0	408.3	408.8	0.30
H_{ce} (Oe)	2.232	2.233	2.230	2.229	2.228	0.002
Tref (nW)	417.1	416.1	408.8	416.0	416.1	3.40
Disp _k 50% (deg)	0.3710	0.3726	0.3776	0.3756	0.3710	0.003
Disk 90% (deg)	1.051	1.055	1.006	1.064	1.051	0.02
Skew (deg)	-	-	0.6015	-	-	0.09
	0.6588	0.5156		0.4583	0.6588	

The standard deviation of the measurements are presented in the last column of the table.

3.2.3. Thickness Measurements of the Plated Film

By laying down five circles of photoresist with 1 mm in diameter, using the mask shown in Figure 12, plating the

wafers, and removing the resist, five steps for thickness measurements were defined. Then a DEKTAK 3030 AUTO II surface profile measuring system was used to monitor the thicknesses of plated film. The measurements on DEKTAK systems are made electromechanically by moving the sample beneath a diamond-tipped stylus⁽¹⁶⁾. The stylus is mechanically coupled to the core of an Linear Variable Differential Transformer(LVDT). An analog signal proportional to the stylus movement is generated by LVDT, which in turn gets digitized in computer memory for display.

In Figure 20 the thickness variation for the plated wafers is shown.

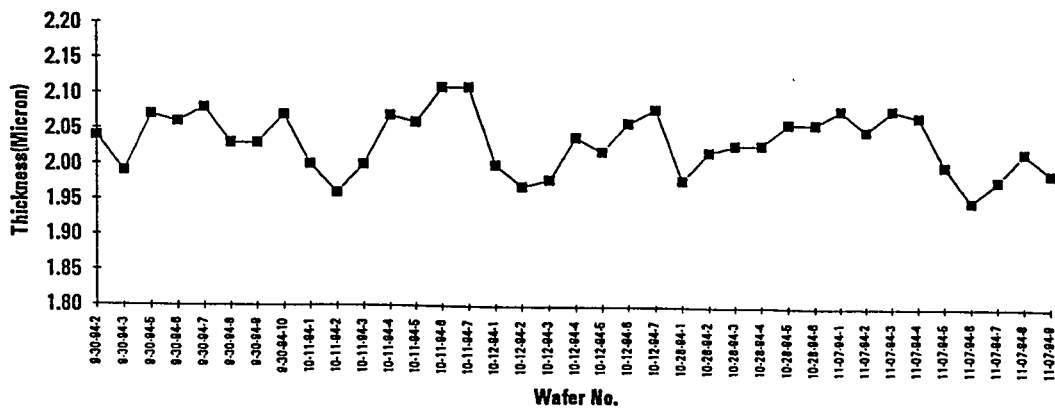


Figure 20. Measured thicknesses for the plated wafers.

Based on the results the typical variation in thickness across a plated wafer is well within $2.0 \pm 0.15 \mu\text{m}$.

3.2.4. Roughness Measurements of the Plated Film

For roughness evaluation, the tapping mode of an Atomic Force Microscope (AFM) was used, and two 7 μm plated CoNiFe film and NiFe plated film were measured. The NiFe film was used as a comparison. The NanoScope III Large Scanning Probe Microscope (LSSPM) was the AFM used for the measurement. The system relies on a laser interference method to detect the deflection of the cantilever. Figure 21 depicts the cantilever deflection detection system and its relationship to the sample.

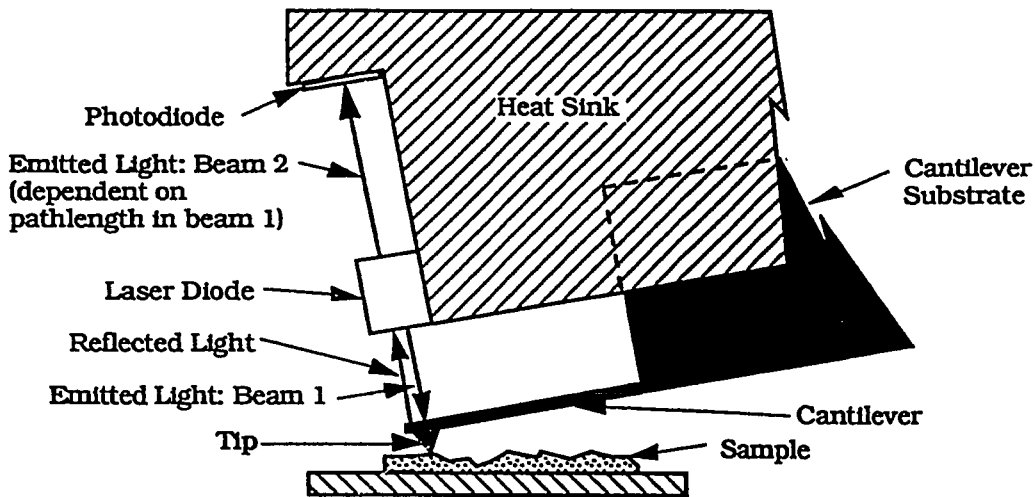


Figure 21. Cantilever Deflection Detection System of the AFM⁽¹⁷⁾.

The roughness analysis of the samples are presented in Figures 22 and 23. As can be seen, the mean roughness of CoNiFe is 42Å in comparison to 62Å for NiFe

3.2.5. Hardness Measurements of the Plated Film

The same samples used for roughness evaluation were used for hardness measurements. Hardness was evaluated by using a BUEHLER MICROMET 3 microhardness tester. The plated film thickness was 7µm, based on the selected gram load, to ensure reliable readings, and the films were plated on the rigid Alsimag(Al2O3+TiC) substrates with 10µm Al2O3 underlayer.

The hardness measurements are presented in Table 9.

Table 9. Hardness measurements of the plated NiFe and CoNiFe.

CoNiFe Hardness (Knoops)	NiFe Hardness (Knoops)
347.7	392.6
305.9	422.9
328.6	447.3
417.2	422.9
397.8	498.9

On the average the Knoop hardness of CoNiFe is 359 while the average Knoop hardness for NiFe is 437.

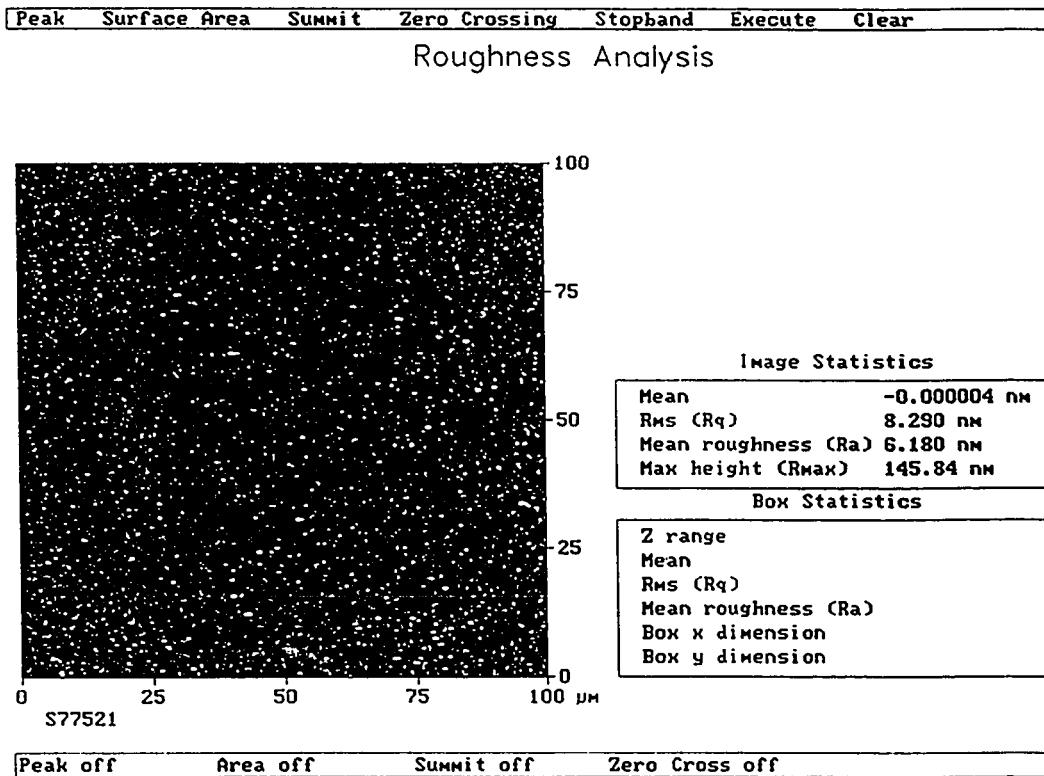
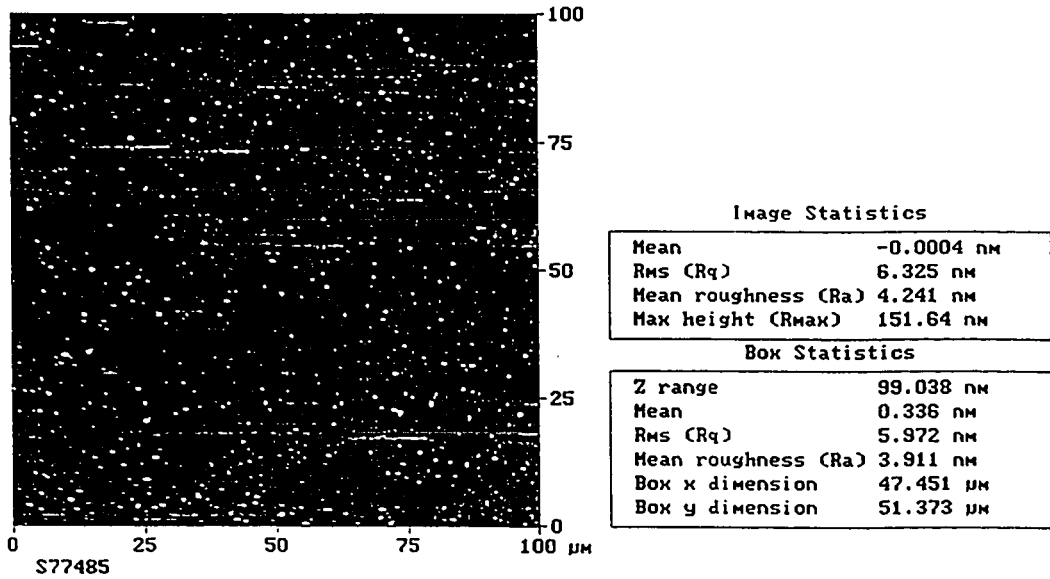


Figure 22. Roughness Analysis of NiFe.

Peak Surface Area Summit Zero Crossing Stopband Execute Clear

Roughness Analysis



Peak off Area off Summit off Zero Cross off

Figure 23. Roughness Analysis of CoNiFe.

3.2.6. Current Density versus Composition and Magnetic Properties

Three test wafers were run for each current density: 3, 4, 5, 6, 7, 8, 9, 11, 13, 15, 20, and 30 mA/cm². As was shown before, the thickness of the wafers was kept within $2.0 \pm 0.2\mu\text{m}$. The current density dependency of the film composition is shown in Figure 24. An increase in current density has increased the proportion of the Fe, the less noble metal, at the expense of Co and to some extent Ni. The data show that increasing the current density from 3 to 30 mA/cm² has increased the Fe by 3.6% along with a decrease of Co by 2.2% and Ni by 1.4%.

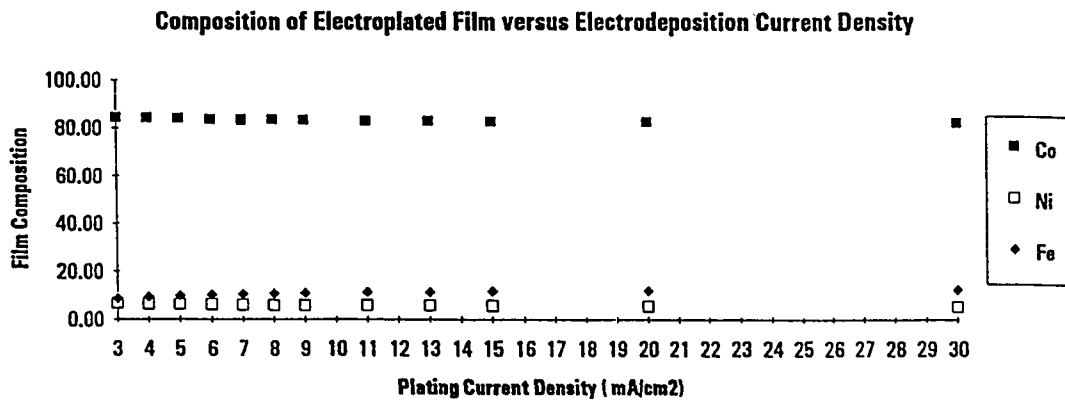


Figure 24. The dependency of current density on the film composition.

B_s , H_k , easy and hard axis coercivity of the plated films versus the electroplating current density are shown in Figures 25, 26, and 27 respectively.

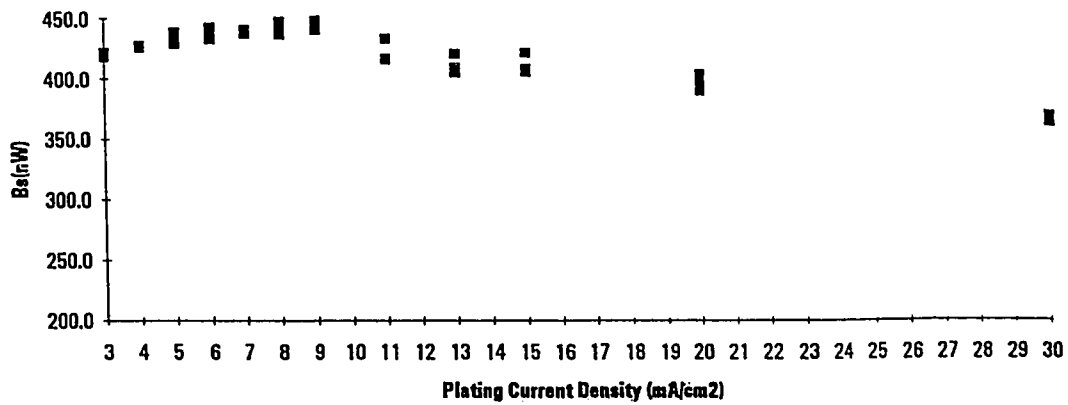


Figure 25. B_s of the plated film verses electrodeposition current density.

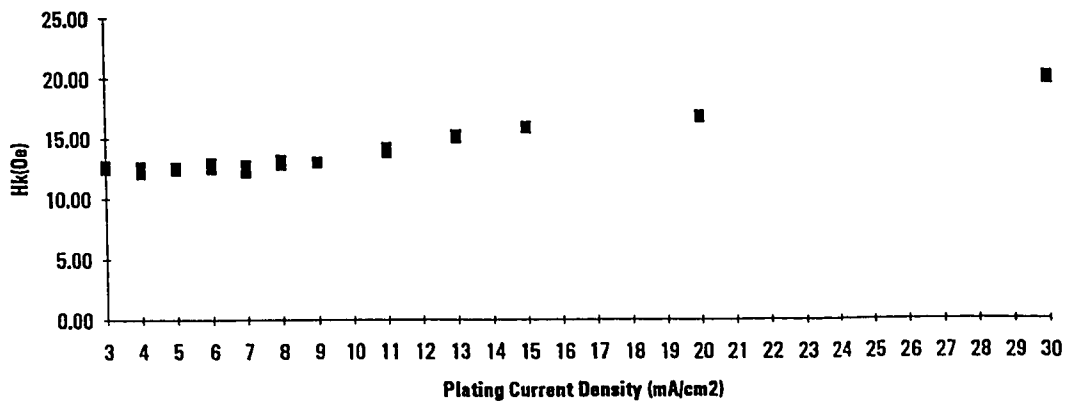


Figure 26. H_k of the plated film verses electrodeposition current density.

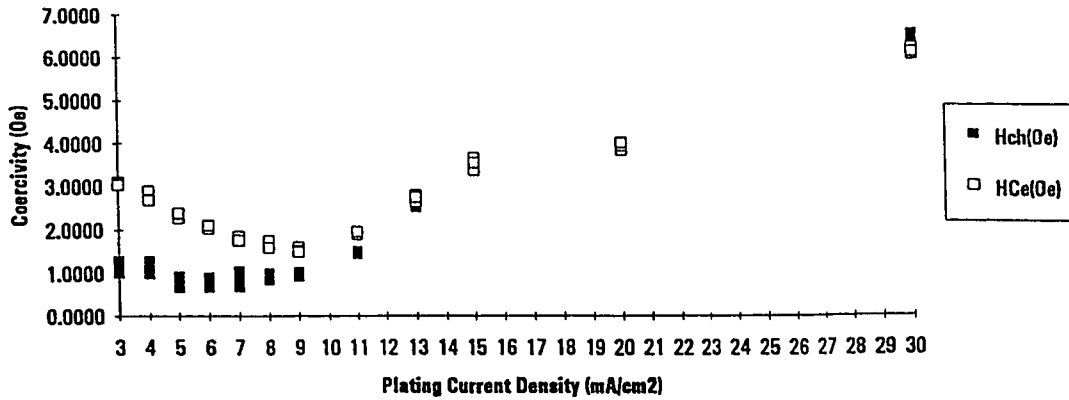


Figure 27. Easy and Hard Axis coercivity versus electrodepositon current density.

Based on the data, it is concluded that 9 mA/cm² is the optimum current density because the B_s is maximum, and H_k , and H_c are minimum. At this current density, $H_k \cong 13$ Oe, $H_{ce} \cong 1$ Oe, $H_{ce} \cong 1.5$ Oe, $B_s \cong 440nW (\cong 16000$ gauss), λ is negative and close to zero. The composition of the film plated at 9mA/cm² is: $Co_{83.4} Ni_{5.7} Fe_{10.9}$, which is the optimum film composition.

3.2.7. XRD and Structural Evaluation

One plated glass test wafer with the optimum composition was sent out for X-ray Diffraction to identify the crystal structure. The XRD chart of the sample is shown in Figure 28. The major peak appeared at 44.5° which indicates that the film consists of a ϵ -Co (0002) hexagonal close-packed (hcp) structure.

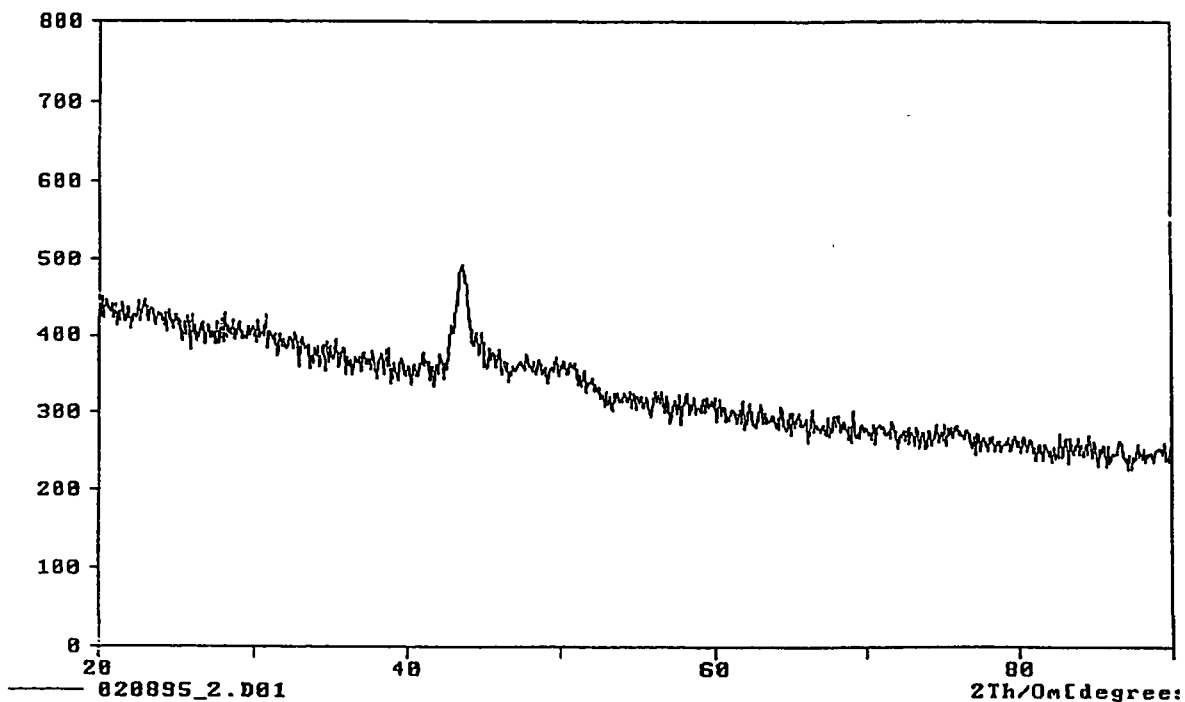


Figure 28. The XRD analysis of the CoNiFe plated film.

3.3. Modification of the Bath and Optimization of the Compositional Gradient across the Topology of Thin Film Structure

Typical topology of the thin film head was shown in Figure 14 previously. The compositional gradients result from the variation in current densities from point to point due to the complex shape of the object being plated⁽⁶⁾. A substantial compositional gradient along the surface of a magnetic recording head element will affect the magnetic recording performance of the head adversely. In NiFe plating, the compositional gradient can be minimized by using a low current density for plating the film⁽⁶⁾. In order to verify this phenomenon for the CoNiFe plating, two wafers with P2 layer topology were plated: one at 9 mA/cm², the desired current density, and the other one at 3 mA/cm², the minimum current density with an acceptable plating efficiency. The EDX analyses of the thin film head after cross sectioning are shown in Figure 29 (refer to P2 layer topology in Figure 3).

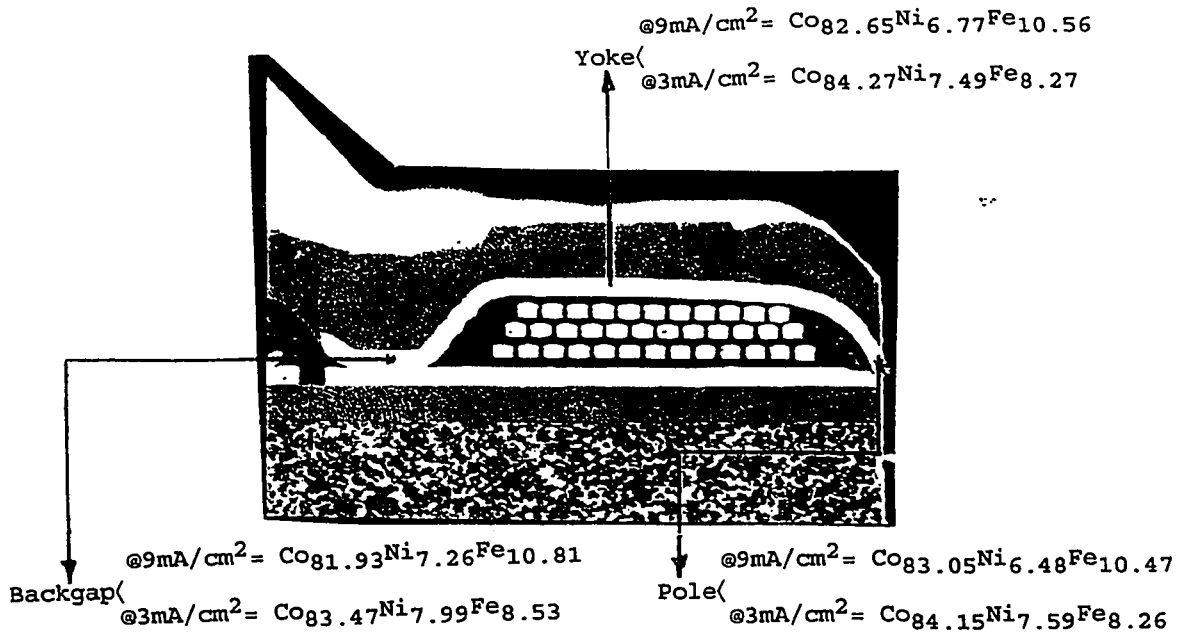


Figure 29. EDX Analyses of the Cross Sections for 3mA/cm² and 9mA/cm².

The data, shown in Figure 29, are the average of 20 samples measured on each wafer. In Table 10 the differences in composition for three parts of the thin film structure, namely: yoke, pole tip, and backgap are shown.

Table 10. The compositional differences for 3 and 9 mA/cm².

	X _{Co} (Yoke)	X _{Ni} (Yoke)	X _{Fe} (Yoke)	X _{Co} (Yoke)	X _{Ni} (Yoke)	X _{Fe} (Yoke)
	-	-	-	-	-	-
	X _{Co} (Pole)	X _{Ni} (Pole)	X _{Fe} (Pole)	X _{Co} (Back-gap)	X _{Ni} (Back-gap)	X _{Fe} (Back-gap)
3mA/cm ²	-0.12	-0.10	0.01	0.80	-0.50	-0.26
9mA/cm ²	0.40	0.29	0.09	0.72	-0.49	-0.25

Based on these results, the uniformity across the topology for 3 mA/cm² is better. This confirms the previous theory that lowering the current density improves the compositional gradient across the topology of the thin film structure.

In order to modify the bath to achieve the optimum composition, i.e. Co_{83.4} Ni_{5.7} Fe_{10.9}, at 3 mA/cm² current density, the methodology shown in Figure 14 was used. First by addition of FeSO₄·7H₂O the amount of Fe was brought up, then by addition of CoSO₄·7H₂O the amount of Co was adjusted. The response of the bath to additions along with all the EDX analyses are shown in Figure 30. The data are presented in appendix A.

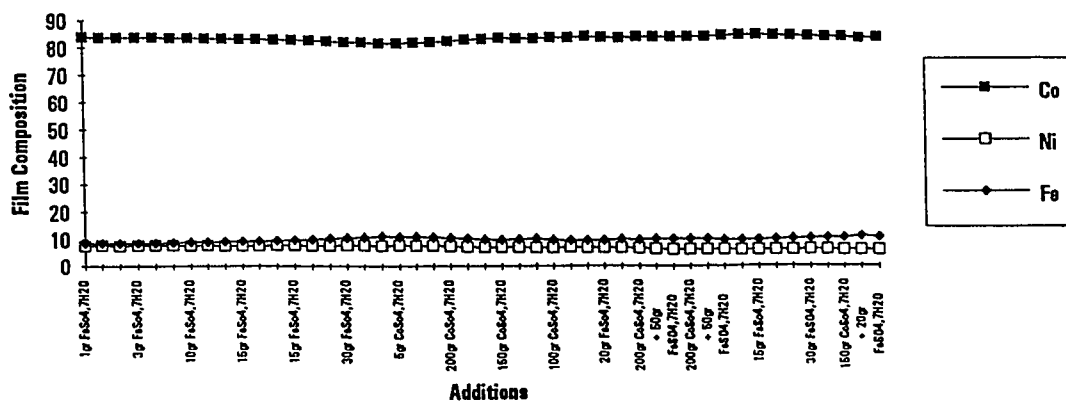


Figure 30. Film composition verses additions during bath modifications.

As is shown, roughly each addition of 10 g of $\text{FeSO}_4 \cdot 7\text{H}_2\text{O}$ increased the Fe by 0.1% , lowers the Co by 0.1%, and each 100 g of $\text{CoSO}_4 \cdot 7\text{H}_2\text{O}$ increased the amount of Co by 0.2%. The concentration of dischargeable ions in the modified bath was: $\text{Co}^{++}=23.8$, $\text{Ni}^{++}=9.6$, $\text{Fe}^{++}=3.6$ g/l.

3.4. The Saturation Magnetostriction (λ_s) Evaluation

By using Equation (2.9) which was presented in Section 2.2.4, the saturation magnetostriction (λ_s) of the plated film with optimum composition was evaluated. The minimum ΔH_k for NiFe, which has been measured by the author is about 0.2 Oe, the measured ratio of $M_{\text{S}_{\text{CoNiFe}}}/M_{\text{S}_{\text{NiFe}}}$ is around 1.61, and the measured ΔH_k for the plated film with optimum composition was 0.32 Oe. By inserting the above value in Equation(2.9), the saturation magnetostriction of the CoNiFe can be related to the saturation magnetostriction of NiFe, as follows:

$$\lambda_{\text{S}_{\text{CoNiFe}}} = 2.6 \lambda_{\text{S}_{\text{NiFe}}} \quad (3.1)$$

4. CONCLUSION

An electroplating bath for fabrication of CoNiFe thin films was developed. The bath was optimized for fabrication of magnetically soft CoNiFe thin films with high saturation magnetization (B_s), low coercivity (H_c), and small magnetostriction constant (λ_s), suitable for the core of thin film heads. The optimum composition was found to be $Co_{83.4}Ni_{5.7}Fe_{10.9}$ with the anisotropy (H_K) \cong 13 Oe, hard axis coercivity (H_{ch}) \cong 1 Oe, easy axis coercivity (H_{ce}) \cong 1.5 Oe, saturation magnetization (B_s) \cong 440nW (\cong 16000 gauss), and small negative saturation magnetostriction coefficient (λ_s). The resulting films were a single Phase with hexagonal close-packed (hcp) structure. The plated films have a roughness of around 42Å and the microhardness of 359 knoops.

The above results lead us to conclude that the CoNiFe ternary alloy electroplated films show promise for use as high- B_s thin film cores in magnetic heads for hard disk devices recording onto high- H_c media.

5. REFERENCES

1. C. D. Mee and E.D. Daniel, Magnetic Recording Vol.II: Computer Data Storage, MacGraw-Hill, p. 6, (1988).
2. J. Bond, "The Incredible Shrinking Disk Drive," *Sol. St. Tech*, p.39, (Sep.1993).
3. S. X. Wang, *Thin Film Recording Heads Using High Moment Soft Magnetic Materials*. PhD thesis, Department of Electrical and Computer Engineering, Carnegie Mellon University, Pittsburg, PA, (1993).
4. N.C. Anderson, R.B. Chesnutt, and G.L. Kaplan, *U.S. Patent 4,661,216* (1987).
5. Y. Omata, "Magnetic Properties of Fe-Co-Ni Films with High Saturation Magnetization Prepared by Evaporation and Electrodeposition," *IEEE Trans. J. Magn. Jap.*, 5(1), 17 (1990).
6. N.C. Anderson, C.R. Grover, Jr, and G.L. Kaplan, *U.S. Patent 4,279,707* (1981).
7. S.C. Srivastava, "Electrodeposition of ternary alloy: developments in 1971-1978," *Surf. Tech.*, 10(4), 237 (1980).
8. C.H. Tolman, "Non-magnetostrictive compositions of Fe-Ni-Co films," *J. Appl. Phys.* 38, 3409 (1967).

9. F. Lowenheim, "Deposition of inorganic films from solutions," in Thin Film Processes, Academic Press, New York, (1978).
10. N. Nakamura and T. Hayashi, " Temperature and pH effects on the anomalous codeposition of Ni-Fe alloys," *Plating and Surface Finishing*, (Aug.1985).
11. D. Fundakowski, *Read-Rite Engineering Education Plating Seminar*, Internal Document. Read Rite Corp., Milpitas, CA, (Jul. 1993).
12. M. Prutton, Thin ferromagnetic films, Butterworth, Washington, p. 83, (1964).
13. Kevex publication " Energy-Dispersive X-ray Microanalysis: An Introduction," *Kevex Instruments publication*, Kevex Instruments, San Carlos, CA, (1989).
14. C.L. Feldman and J.W. Mayer, Fundamentals of Surface and thin film analysis, North-Holland, p.167, (1986).
15. C.B. Boss and K.J. Fredeen, "Concepts, Instrumentation, and Techniques in Inductively Coupled Plasma Atomic Emission Spectrometry," *Perkin-Elmer Corporation Publication* (1989).
16. *DEKTAK 3030 Auto II programmable stage profiler technical manual*, Veeco Instruments Inc., Sloan Technology Division, Santa Barbara, CA.
17. *Large Sample Scanning Probe Microscope User's Manual*, Digital Instruments, Version 1.2, (May 1993).

6. Appendix A. EDX data on bath modification

Table 11. EDX data and the additions of bath modification

EDX (CoNiFe)	Addition
Co=83.98, Ni=7.57, Fe=8.45	1gr FeSo4, 7H2O
Co=83.88, Ni=7.65, Fe=8.47	2gr FeSo4, 7H2O
Co=83.91, Ni=7.55, Fe=8.54	2gr FeSo4, 7H2O
Co=83.80, Ni=7.65, Fe=8.55	3gr FeSo4, 7H2O
Co=83.86, Ni=7.61, Fe=8.54	5gr FeSo4, 7H2O
Co=83.62, Ni=7.67, Fe=8.72	10gr FeSo4, 7H2O
Co=83.57, Ni=7.59, Fe=8.84	10gr FeSo4, 7H2O
Co=83.35, Ni=7.76, Fe=8.89	5gr FeSo4, 7H2O
Co=83.45, Ni=7.58, Fe=8.97	5gr FeSo4, 7H2O
Co=83.19, Ni=7.60, Fe=9.21	15gr FeSo4, 7H2O
Co=83.21, Ni=7.52, Fe=9.27	15gr FeSo4, 7H2O
Co=82.97, Ni=7.63, Fe=9.39	15gr FeSo4, 7H2O
Co=82.79, Ni=7.62, Fe=9.59	15gr FeSo4, 7H2O
Co=82.59, Ni=7.54, Fe=9.87	20gr FeSo4, 7H2O
Co=82.27, Ni=7.59, Fe=10.15	30gr FeSo4, 7H2O
Co=81.89, Ni=7.65, Fe=10.46	30gr FeSo4, 7H2O
Co=81.75, Ni=7.57, Fe=10.68	20gr FeSo4, 7H2O
Co=81.53, Ni=7.54, Fe=10.93	10gr FeSo4, 7H2O
Co=81.53, Ni=7.66, Fe=10.80	5gr CoSo4, 7H2O
Co=81.66, Ni=7.49, Fe=10.86	20gr CoSo4, 7H2O
Co=81.87, Ni=7.51, Fe=10.62	100gr CoSo4, 7H2O
Co=82.32, Ni=7.29, Fe=10.39	200gr CoSo4, 7H2O
Co=82.75, Ni=7.09, Fe=10.18	315gr CoSo4, 7H2O
Co=83.13, Ni=6.94, Fe=9.93	200gr CoSo4, 7H2O
Co=83.39, Ni=6.86, Fe=9.75	150gr CoSo4, 7H2O
Co=83.24, Ni=6.84, Fe=9.92	20gr FeSo4, 7H2O
Co=83.19, Ni=6.78, Fe=10.03	10gr FeSo4, 7H2O
Co=83.53, Ni=6.75, Fe=9.71	100gr CoSo4, 7H2O
Co=83.66, Ni=6.86, Fe=9.48	100gr CoSo4, 7H2O
Co=83.93, Ni=6.69, Fe=9.37	100gr CoSo4, 7H2O
Co=83.66, Ni=6.78, Fe=9.56	20gr FeSo4, 7H2O
Co=83.47, Ni=6.64, Fe=9.89	30gr FeSo4, 7H2O
Co=83.80, Ni=6.45, Fe=9.75	300gr CoSo4, 7H2O + 30gr FeSO4, 7H2O
Co=83.75, Ni=6.28, Fe=9.97	200gr CoSo4, 7H2O + 50gr FeSO4, 7H2O
Co=83.79, Ni=6.11, Fe=10.10	300gr CoSo4, 7H2O + 40gr FeSO4, 7H2O
Co=83.90, Ni=6.15, Fe=9.95	50gr CoSo4, 7H2O + 10gr FeSO4, 7H2O
Co=83.91, Ni=6.04, Fe=10.05	200gr CoSo4, 7H2O + 50gr FeSO4, 7H2O
Co=84.24, Ni=6.03, Fe=9.73	100gr CoSo4, 7H2O
Co=84.47, Ni=5.94, Fe=9.59	15gr FeSo4, 7H2O
Co=84.36, Ni=5.93, Fe=9.70	15gr FeSo4, 7H2O
Co=84.28, Ni=5.93, Fe=9.79	25gr FeSo4, 7H2O
Co=84.04, Ni=6.00, Fe=9.96	30gr FeSo4, 7H2O
Co=83.74, Ni=6.11, Fe=10.16	30gr FeSO4, 7H2O
Co=83.54, Ni=6.04, Fe=10.41	50gr CoSo4, 7H2O + 40gr FeSO4, 7H2O
Co=83.54, Ni=5.96, Fe=10.51	40gr CoSo4, 7H2O + 40gr FeSO4, 7H2O
Co=83.12, Ni=5.97, Fe=10.97	150gr CoSo4, 7H2O + 20gr FeSO4, 7H2O
Co=83.44, Ni=5.94, Fe=10.62	